CHAPTER 4
NONLINEAR VIBRATION

Fredric Ehrich
H. Norman Abramson

INTRODUCTION

A vast body of scientific knowledge has been developed over a long period of time devoted to a description of natural phenomena. In the field of mechanics, rapid progress in the past two centuries has occurred, due in large measure to the ability of investigators to represent physical laws in terms of rather simple equations. In many cases the governing equations were not so simple; therefore, certain assumptions, more or less consistent with the physical situation, were employed to reduce the equations to types more easily soluble. Thus, the process of linearization has become an intrinsic part of the rational analysis of physical problems. An analysis based on linearized equations, then, may be thought of as an analysis of a corresponding but idealized problem.

In many instances the linear analysis is insufficient to describe the behavior of the physical system adequately. In fact, one of the most fascinating features of a study of nonlinear problems is the occurrence of new and totally unsuspected phenomena; i.e., new in the sense that the phenomena are not predicted, or even hinted at, by the linear theory. On the other hand, certain phenomena observed physically are unexplainable except by giving due consideration to nonlinearities present in the system.

The branch of mechanics that has been subjected to the most intensive attack from the nonlinear viewpoint is the theory of vibration of mechanical and electrical systems. Other branches of mechanics, such as incompressible and compressible fluid flow, elasticity, plasticity, wave propagation, etc., also have been studied as nonlinear problems, but the greatest progress has been made in treating vibration of nonlinear systems. The systems treated in this chapter are systems with a finite number of degrees-of-freedom which can be defined by a finite number of simultaneous ordinary differential equations; on the other hand, the mechanics of continua involves partial differential equations. Nonlinear ordinary differential equations are easier to handle than nonlinear partial differential equations. An interesting survey of the entire realm of nonlinear mechanics is given in Ref. 1.

This chapter provides information concerning features of nonlinear vibration theory likely to be encountered in practice and methods of nonlinear vibration analysis which find ready application.

EXAMPLES OF SYSTEMS POSSESSING NONLINEAR CHARACTERISTICS

SIMPLE PENDULUM

As a first example of a system possessing nonlinear characteristics, consider a simple pendulum of length l having a bob of mass m, as shown in Fig. 4.1. The well-known differential equation governing free vibration is

$$ml^2\ddot{\theta} + mgl\theta = 0 \tag{4.1}$$

This equation holds only for small oscillations about the position of equilibrium since the actual restoring moment is characterized by the quantity $\sin\theta$. Equation (4.1) thus employs the assumption $\sin\theta \simeq \theta$. The exact, but nonlinear, equation of motion is

$$ml^2\ddot{\theta} + mgl \sin\theta = 0 \tag{4.2}$$

SIMPLE SPRING-MASS SYSTEM

A simple spring-mass system, as shown in Fig. 4.2, is characterized by the equation

$$m\ddot{x} + kx = 0$$

This equation is based on the assumption that the elastic spring obeys Hooke's law; i.e., the characteristic curve of restoring force versus displacement is a straight line. However, many materials do not exhibit such a linear characteristic. Further, in the case of a simple coil spring, a deviation from linearity occurs at large compression as the coils begin to close up, or conversely, when the extension becomes so great that the coils begin to lose their individual identity. In either case, the spring exhibits a characteristic such that the restoring force increases more rapidly than the displacement. Such a characteristic is called *hardening.* In a similar manner, certain systems (e.g., a simple pendulum) exhibit a *softening* characteristic. Both types of characteristic are shown in Fig. 4.3. A simple system with either softening or hardening restoring force may be described approximately by an equation of the form

$$m\ddot{x} + k(x \pm \mu^2 x^3) = 0$$

where the upper sign refers to the hardening characteristic and the lower to the softening characteristic.

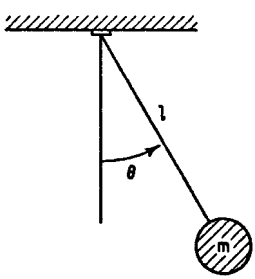

FIGURE 4.1 Simple pendulum.

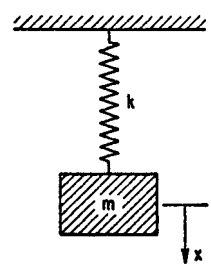

FIGURE 4.2 Simple spring-mass system.

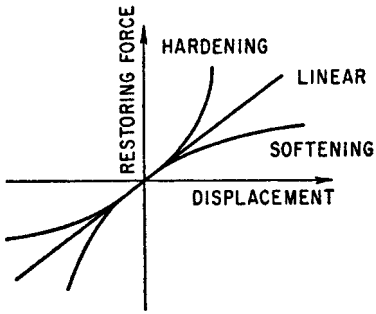

FIGURE 4.3 Restoring force characteristic curves for linear, hardening, and softening vibration systems.

It is possible for a system with only linear components to exhibit nonlinear characteristics, by snubber action for example, as shown in Fig. 4.4. A system undergoing vibration of small amplitude also may exhibit nonlinear characteristics; for example, in the pendulum shown in Fig. 4.5, the length depends on the amplitude.

STRETCHED STRING WITH CONCENTRATED MASS

The large amplitude vibration of a stretched string with a concentrated mass, as shown in Fig. 4.6, offers another example of a nonlinear system. The governing nonlinear differential equation is, approximately,

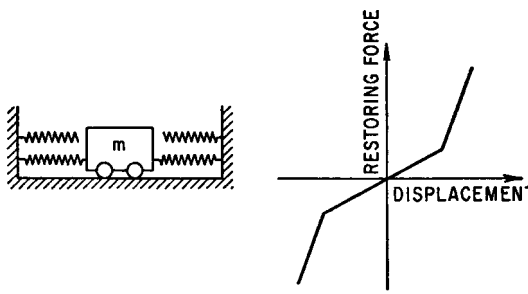

FIGURE 4.4 Nonlinear mechanical system with snubber action showing piecewise linear restoring force characteristic curve.

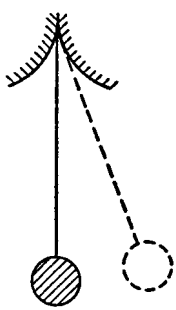

FIGURE 4.5 Pendulum with nonlinear characteristic resulting from dependence of length on vibration amplitude.

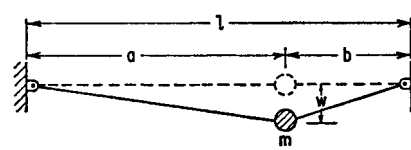

FIGURE 4.6 Vibration of a weighted string as an example of a nonlinear system.

$$m\ddot{w} + F_0\left(\frac{l}{ab}\right)w + (SE - F_0)\left(\frac{a^3 + b^3}{2a^3b^3}\right)w^3 = 0$$

where F_0 is the initial tension, S is the cross-sectional area, and E is the elastic modulus of the string. Consider now the special case of $a = b$ and denote the unstretched length of the half string by l_0. Then the initial tension and the restoring force become

$$F_0 = SE\left(\frac{a - l_0}{l_0}\right)$$

$$F_r \simeq SE\left[2\left(\frac{a}{l_0} - 1\right)\left(\frac{w}{a}\right) + \left(2 - \frac{a}{l_0}\right)\left(\frac{w}{a}\right)^3\right]$$

An interesting feature of this system is that it exhibits a wide variety of either hardening or softening characteristics, depending upon the value of a/l_0, as shown in Fig. 4.7.

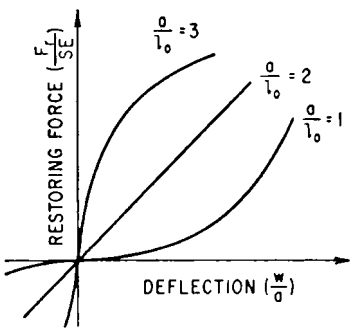

FIGURE 4.7 Restoring force characteristics for the weighted string shown in Fig. 4.6.

SYSTEM WITH VISCOUS DAMPING

The foregoing examples all involve nonlinearities in the elastic components, either as a result of appreciable amplitudes of vibration or as a result of peculiarities of the elastic element. Consider a simple spring-mass system which also includes a dashpot. The usual assumptions pertaining to this system are that the spring is linear and that the motion is sufficiently slow that the viscous resistance provided by the dashpot is proportional to the velocity; therefore, the governing equation of motion is linear. Frequently, the dashpot resistance is more correctly expressed by a term proportional to the square of the velocity. Further, the resistance is always such as to oppose the motion; therefore, the nonlinear equation of motion may be written

$$m\ddot{x} + c|\dot{x}|\dot{x} + kx = 0$$

BELT FRICTION SYSTEM

The system shown in Fig. 4.8*A* involves a nonlinearity depending upon the dry friction between the mass and the moving belt. The belt has a constant speed v_0, and the applicable equation of motion is

$$m\ddot{x} + F(\dot{x}) + kx = 0$$

where the friction force $F(\dot{x})$ is shown in Fig. 4.8*B*. For large values of displacement, the damping term is positive, has positive slope, and removes energy from the sys-

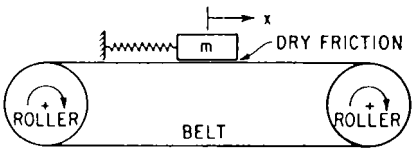

FIGURE 4.8*A* Belt friction system which exhibits self-excited vibration.

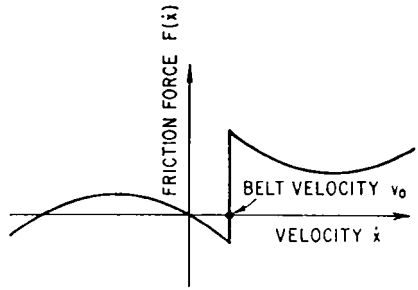

FIGURE 4.8*B* Damping force characteristic curve for the belt friction system shown in Fig. 4.8*A*.

tem; for small values of displacement, the damping term is negative, has negative slope, and actually puts energy into the system. Even though there is no external stimulus, the system can have an oscillatory solution, and thus corresponds to a nonlinear *self-excited* system. (See Chap. 5.)

SYSTEMS WITH ASYMMETRIC STIFFNESS

The aforementioned examples of nonlinear stiffness, typified by the stiffness variations in Figs. 4.3, 4.4, and 4.7, all may be characterized as symmetric. That is, the variation in the absolute value of the restoring force with displacement in the positive direction is identical to the variation in the absolute value of the restoring force with displacement in the negative direction. As will be seen in the following sections, symmetric stiffness distributions result in changes in the shape of the resonant peak of the response curve and slight distortion in the waveform of the dynamic motion without changing the basic synchronism between forcing function and response. But many more diverse phenomena and much more profound changes are encountered when dealing with asymmetric stiffness distributions.

A typical physical situation is encountered in the dynamics of rotating machinery where a softly mounted rotor is located eccentrically within the small clearance of a motion limiting stiff stator as illustrated in Fig. 4.9*A* and *C*. When rotating with some unbalance in the rotor, the vertical component of the unbalance force will cause intermittent local contact with the stiff stator, resulting in a "bouncing" motion of the rotor. The stiffness characteristic for the vertical motion is asymmetric. In its simplest form, it may be represented as a bilinear relationship—very soft for vertical motion in the upward direction and very stiff for vertical motion in the downward direction, as illustrated in Fig. 4.9*B*. More explicitly,

$$k = K_1 \qquad x > 0$$

$$k = K_2 \qquad x < 0$$

Many other examples of nonlinear systems are given in the references of this chapter.

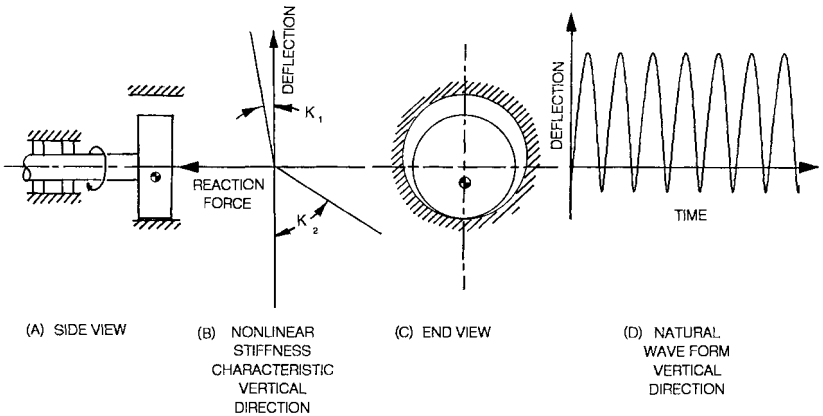

FIGURE 4.9 Nonlinear spring characteristic of a rotor operating with local intermittent contact in a clearance.

DESCRIPTION OF NONLINEAR PHENOMENA

This section describes briefly, largely in nonmathematical terms, certain of the more important features of nonlinear vibration. Further details and methods of analysis are given later.

FREE VIBRATION

Insofar as the free vibration of a system is concerned for systems with symmetric stiffness distributions, one distinguishing feature between linear and nonlinear behavior is the dependence of the period of the motion in nonlinear vibration on the amplitude. For example, the simple pendulum of Fig. 4.1 may be analyzed on the basis of the linearized equation of motion, Eq. (4.1), from which it is found that the period of the vibration is given by the constant value $\tau_o = 2\pi/\omega_n$. An analysis on the basis of the nonlinear equation of motion, Eq. (4.2), leads to an expression for the period of the form

$$\frac{\tau}{\tau_o} = 1 + \tfrac{1}{4}(U)^2 + \tfrac{9}{64}(U)^4 + \tfrac{25}{256}(U)^6 + \cdots \tag{4.3}$$

where U is related to the amplitude of the vibration Θ by the relation $U = \sin(\Theta/2)$. The linear solution thus corresponds to the first term of Eq. (4.3). The dependence of the period of vibration on amplitude is shown in Fig. 4.10. Systems in which the period of vibration is independent of the amplitude are called *isochronous,* while those in which the period τ is dependent on the amplitude are called *nonisochronous.*

The dependence of period on amplitude also may be seen from the vibration trace shown in Fig. 4.11, which corresponds to a solution of the equation

$$m\ddot{x} + c\dot{x} + k(x + \mu^2 x^3) = 0$$

For systems with asymmetric stiffness distributions, free undamped vibration will display significant distortion of the natural waveform. The simple bilinear stiffness

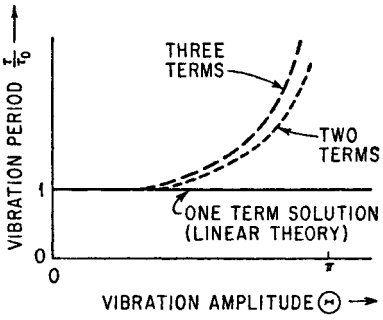

FIGURE 4.10 Period of free vibration of a simple pendulum according to Eq. (4.3) and showing the effect of nonlinear terms.

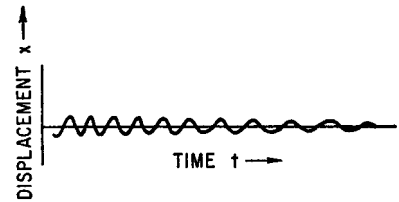

FIGURE 4.11 Deflection time-history for free damped vibration of the nonlinear system described by Duffing's equation [Eq. (4.16)].

distribution of Fig. 4.9*B* will result in the system having a simple harmonic half cycle at relatively low frequency for upward motion and a simple harmonic half cycle at relatively high frequency for downward motion. The overall waveform is then a combination of these two disparate half cycles as represented in Fig. 4.9*D* and suggests a bouncing motion.

RESPONSE CURVES FOR FORCED VIBRATION OF SYSTEMS WITH SYMMETRIC STIFFNESS

Representations of vibration behavior in the form of curves of response amplitude versus exciting frequency are called *response curves.* The response curves for an undamped linear system acted on by a harmonic exciting force of amplitude p and frequency ω may be derived from the equation of motion

$$\ddot{x} + \omega_n^2 x = \frac{p}{m} \cos \omega t \tag{4.4}$$

The solution has the form shown in Fig. 4.12. The vertical line at $\omega = \omega_n$ corresponds not only to resonance but also to free vibration ($p = 0$); the amplitude in this instance is determined by the initial conditions of the motion. In a nonlinear system the character of the motion is dependent upon the amplitude. This requires that the natural frequency likewise be amplitude-dependent; hence, it follows that the free vibration curve $p = 0$ for nonlinear systems cannot be a straight line. Figure 4.13 shows free vibration curves (i.e., natural frequency as a function of amplitude) for hardening and softening systems.

Figures 4.12 and 4.13 suggest that the forced vibration response curves for systems with nonlinear restoring forces have the general form of those of a linear system but are "swept over" to the right or left, depending on whether the system is hardening or softening. These are shown in Fig. 4.14. The principal effect of damping in forced vibration of a nonlinear system is to limit the amplitude at resonance, as shown in Fig. 4.15.

These rightward- and leftward-leaning resonant response peaks have special meaning to the dynamic response of the system. Consider a hardening system whose response curve is shown in Fig. 4.15*B.* Suppose that the exciting frequency starts at a low value, and increases continuously at a slow rate. The amplitude of the vibration

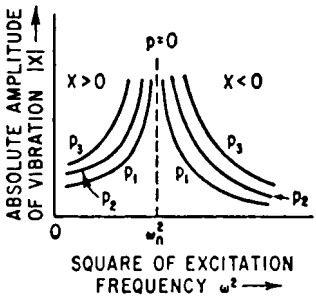

FIGURE 4.12 Family of response curves for the undamped linear system defined by Eq. (4.4).

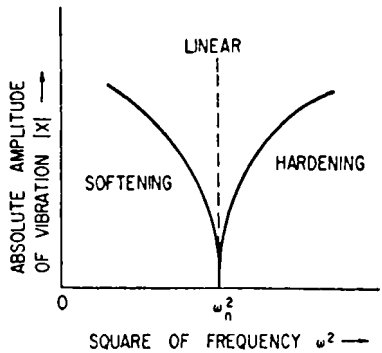

FIGURE 4.13 Free vibration curves (natural frequency as a function of amplitude) in the response diagram for linear, hardening, and softening vibration systems [see Eq. (4.49)].

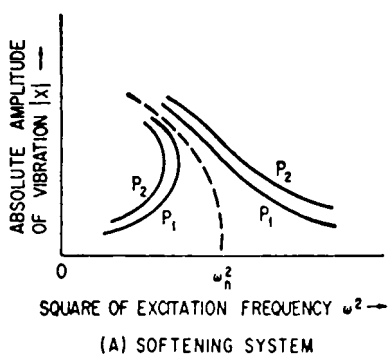

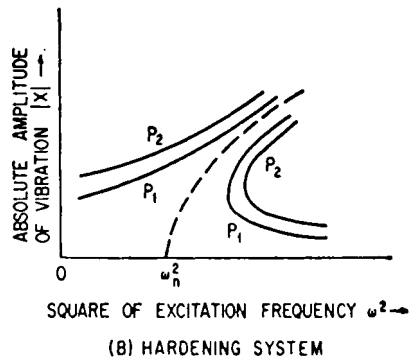

FIGURE 4.14 Response curves for undamped nonlinear systems with hardening and softening restoring force characteristics [see Eq. (4.50)].

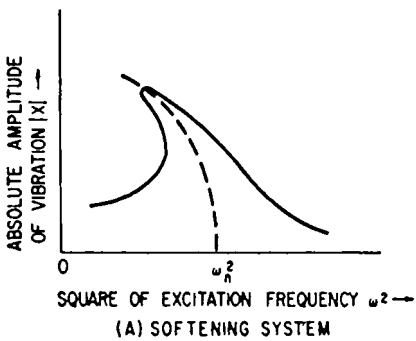

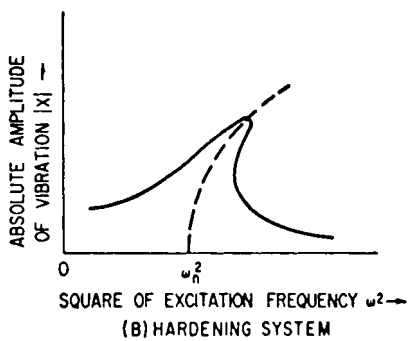

FIGURE 4.15 Response curves for damped nonlinear systems with hardening and softening restoring force characteristics [see Eq. (4.52)].

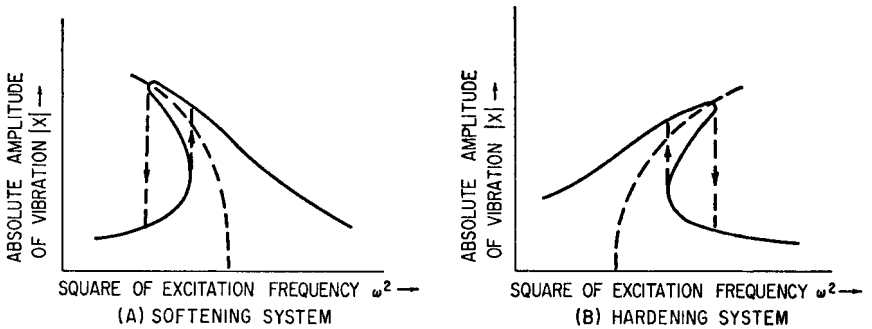

FIGURE 4.16 Jump phenomenon in hardening and softening systems.

also increases, but only up to a point. In particular, at the point of vertical tangency of the response curve, a slight increase in frequency requires that the system perform in an unusual manner; i.e., that it "jump" down in amplitude to the lower branch of the response curve. This experiment may be repeated by starting with a large value of exciting frequency but requiring that the forcing frequency be continuously reduced. A similar situation again is encountered; the system must jump up in amplitude in order to meet the conditions of the experiment. This *jump phenomenon* is shown in Fig. 4.16 for both the hardening and softening systems.[2] The jump is not instantaneous in time but requires a few cycles of vibration to establish a steady-state vibration at the new amplitude.

There is a portion of the response curve which is "unattainable"; it is not possible to obtain that particular amplitude by a suitable choice of forcing frequency. Thus, for certain values of ω there appear to be three possible amplitudes of vibration but only the upper and lower can actually exist. If by some means it were possible to initiate a steady-state vibration with just the proper amplitude and frequency to correspond to the middle branch, the condition would be unstable; at the slightest disturbance the motion would jump to either of the other two states of motion. The direction of the jump depends on the direction of the disturbance. Thus, of the three possible states of motion, one in phase and two out-of-phase with the exciting force, the one having the larger amplitude of the two out-of-phase motions is unstable. This region of instability in the response diagram is defined by the loci of vertical tangents to the response curves, and is shown for a hardening system in Fig. 4.16*C*.

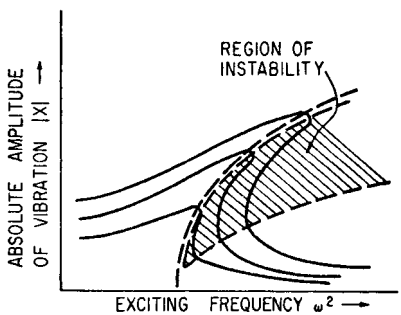

FIGURE 4.16*C* Instability region defined by the loci of vertical tangents of the damped response curves for the hardening system.

RESPONSE CURVES FOR FORCED VIBRATION OF SYSTEMS WITH ASYMMETRIC STIFFNESS

The system pictured in Fig. 4.9 is typical of systems with asymmetric stiffness characteristics, and its response[3,4] in-

cludes a variety of phenomena, including regions of chaotic response,[1] not observed in systems with symmetric stiffness characteristics.

The equations of motion in the plane normal to the plane of contact, with a stiffness of k_1 when the rotor is deflected from its rest position in the soft direction and a stiffness k_2 when the rotor is deflected from its rest position in the hard direction, may be integrated numerically using a simple trapezoidal integration procedure. The rest position of the rotor is taken at the contact point, so the break point of the bilinear elastic characteristic is at zero deflection. The system is then simply characterized by only two parameters—the ratio of the stiffnesses $\beta = k_1/k_2$ and z_1, the linear damping ratio of the system referred to critical damping of the soft system—when operated at a given rotational speed *s,* which is taken in normalized format as the ratio of rotational frequency to the system natural frequency.

For typical values and z_1 and β at any speed *s,* the numerical model may be used to compute the orbit of the rotor mass point as the orthogonal coordinates of the motion *X* and *Y,* where each of the coordinates is normalized as the ratio of the deflection from the rest position to the unbalance mass eccentricity. In considering the response over a large range of rotational speed, the motion may be simply characterized at any particular speed as Y_p, the local peak value(s) of the normalized amplitude in the direction of the nonlinear stiffness. As shown in Fig. 4.17*A* in comparison with the response of an equivalent system with a linear spring support stiffness, a plot of this parameter over a range of speeds is quite effective in detecting and identifying various different response phenomena.

Superharmonic Response.[5,6] Fig. 4.17*B* characterizes superharmonic response at subcritical speed. Shown here at approximately one-half critical speed, the rotor is bouncing at approximately its natural frequency against the hard surface of the

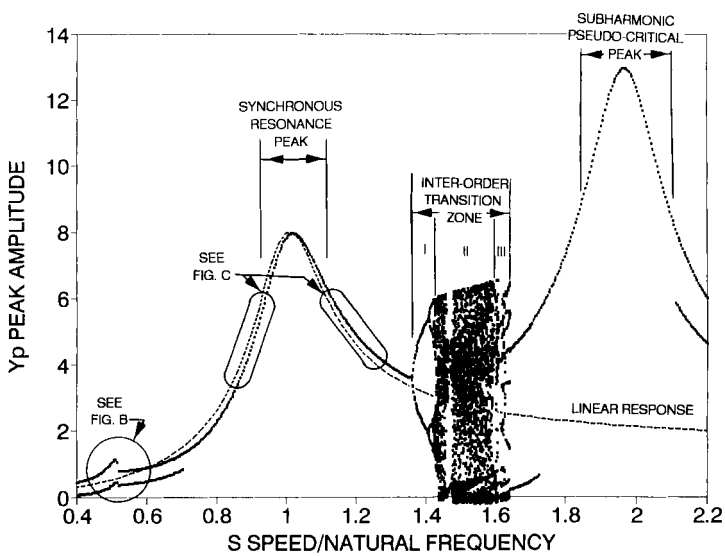

FIGURE 4.17*A* Identification of various classes of nonlinear behavior in the peak amplitude response curve—typical subcritical/critical/supercritical regime ($z_1 = 0.200; \beta = 0.002$).

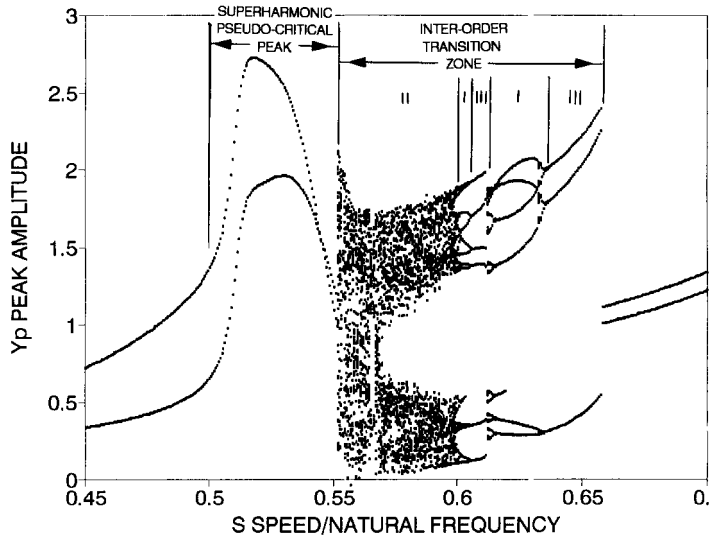

FIGURE 4.17*B* Identification of various classes of nonlinear behavior in the peak amplitude response curve—detail of superharmonic pseudo-critical peak and interorder transition zone ($z_1 = 0.05; \beta = 0.005$).

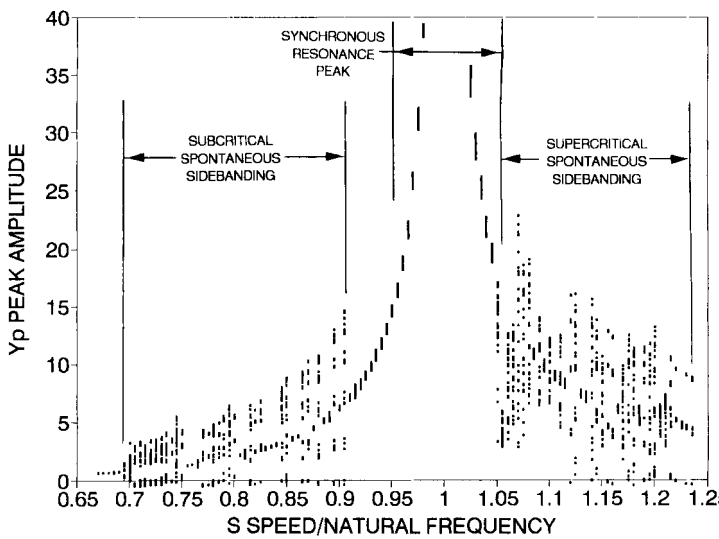

FIGURE 4.17*C* Identification of various classes of nonlinear behavior in the peak amplitude response curve—detail of transcritical spontaneous sidebanding ($z_1 = 0.002; \beta = 0.002$).

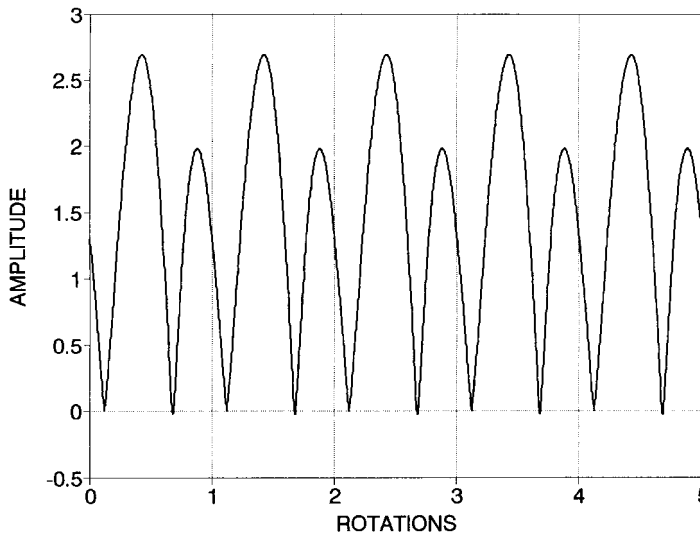

FIGURE 4.18 Subcritical superharmonic response—waveform ($z_1 = 0.050$; $\beta = 0.005$; $s = 0.525$; $M = 2$).

contact point, energized at every other bounce by the component of the unbalance centrifugal force as suggested in Fig. 4.18. The dominant frequency of the response is then precisely 2 times operating speed. Such a pseudo-critical speed is possible for any integer order M at approximately $1/M$ times critical speed and with a significant frequency component of precisely M times operating speed or approximately equal to the *natural frequency.*

Transition between Successive Superharmonic Orders.[6] In between the successive superharmonic response zones (i.e., between the Mth and $(M - 1)$th order superharmonic responses) there may occur a regime of irregular response. Most commonly, the response may be chaotic, as identified as Zone II in Fig. 4.17*B* and shown in Fig. 4.19*A.* For such chaotic motion, the Poincaré section, which is a stroboscopic view of the phase-plane plot of velocity versus displacement at a reference angle of shaft rotation, is effectively a slice of the system's attractor as shown in Fig. 4.19*B.* The chaotic motion may be preceded on one side by a cascade of period-doubling bifurcations in the trace of peak amplitude Y_p, as suggested in Zone I of Fig. 4.17*B.* Another pattern of transition response is periodic in waveform. As shown in Zone III of Fig. 4.17*B,* instead of having an unending series of local peaks with no identifiable periodicity of repetitions as would be the case in truly chaotic motion, the response appears to have clusters of K bounces that actually repeat every L rotations to give a major periodicity of K/L times s. In both the chaotic and periodic transition zones, the response has a significant component at or near the system's *natural frequency.*

Ultra-Subharmonic Response in Transcritical Response (Subcritical).[7,8] A unique response has been identified which appears in very lightly damped, highly nonlinear systems operating in the transcritical range, as shown in Fig. 4.17*C.* It has been observed that one of the dominant sidebands occurs at approximately critical frequency, and the sideband separation is generally a whole-number fraction $|1/(J + 1)|$ of

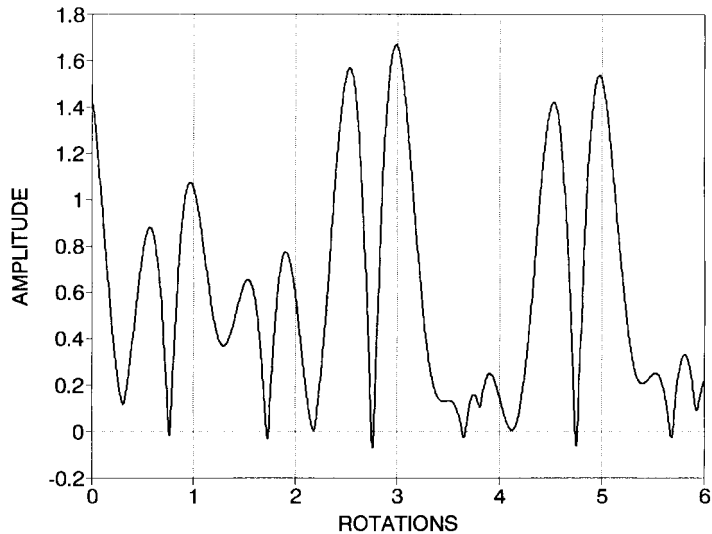

FIGURE 4.19*A* Subcritical chaotic transition between successive superharmonic orders—waveform ($z_1 = 0.050$; $\beta = 0.005$; $s = 0.560$; $2 < M < 1$).

the operating speed and, in the *J*th order manifestation (that is, $J = -1, -2, -3, \ldots$) of subcritical spontaneous sidebanding when the speed is approximately $(J + 1)/J$ times the natural frequency, the dominant frequency is precisely $J/(J + 1)$ times the rotative speed or approximately equal to the *natural frequency.* The waveform, shown in Fig. 4.20, is periodic in nature. There appear to be transition zones between succes-

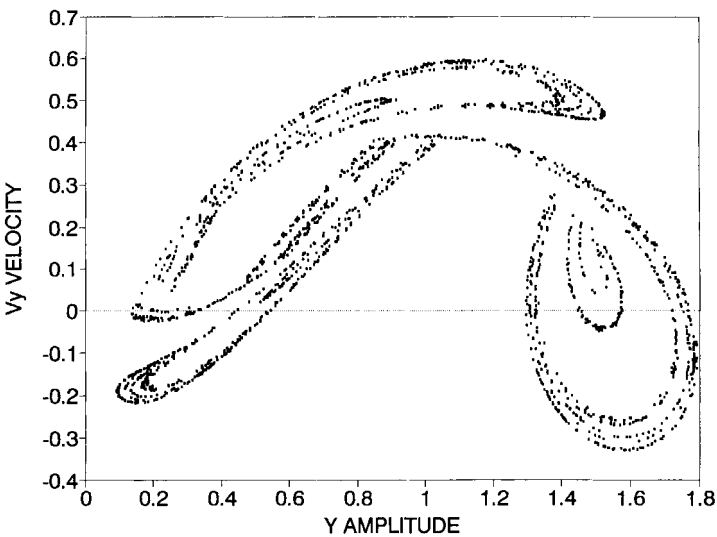

FIGURE 4.19*B* Subcritical chaotic transition between successive superharmonic orders—Poincaré section ($z_1 = 0.050$; $\beta = 0.005$; $s = 0.560$; $2 < M < 1$).

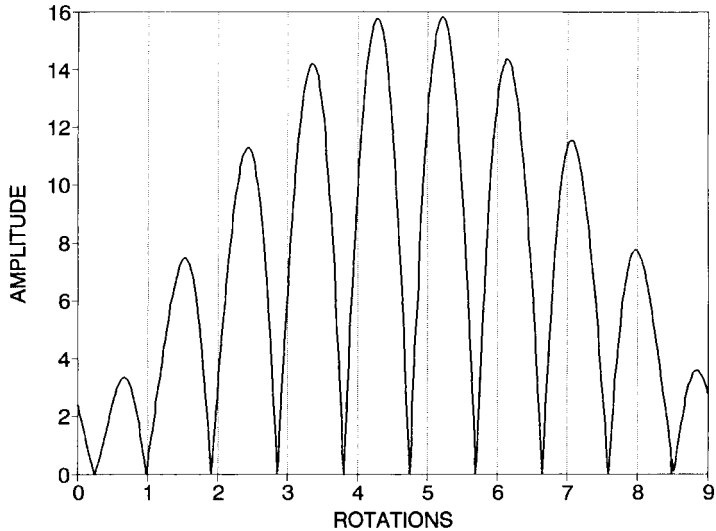

FIGURE 4.20 Transcritical spontaneous sidebanding—waveform ($z_1 = 0.001; \beta = 0; s = 0.900; J = -10$).

sive orders of J when the response has a dominant frequency approximately equal to the system's *natural frequency* and the waveform may be chaotic. The general phenomenon has been referred to as *ultra-subharmonic response.* It has also been called *spontaneous sidebanding* because the sidebands appear around the center forcing frequency without the presence of and interaction with a second external forcing frequency. In a more general formulation,[9] it has been noted that such ultra-subharmonic response can be found in a speed range just below the Mth-order subharmonic peak at a rotational speed which is approximately $(MJ + 1)/J$ times the natural frequency (where $J = -1, -2, -3, \ldots$) with a dominant response frequency precisely equal to $J/(MJ + 1)$ times the rotational speed.

Synchronous Resonant Response. Synchronous critical response in the nonlinear system, shown in Fig. 4.17*A,* is very similar to that of the linear system except for the distortion of the waveform reflecting the bouncing nature of the motion illustrated in Fig. 4.21. Although the dominant frequency component is that of the forcing frequency or operating speed which is close to the *natural frequency* of the system, the bouncing waveform produces significant spectral content at whole number multiples of the operating speed.

Ultra-Subharmonic Response in Transcritical Response (Supercritical).[8] As shown in Fig. 4.17*C,* ultra-subharmonic response or spontaneous sidebanding can occur at speeds slightly higher than critical speed, very similar in nature to the response already noted above which occurs at slightly subcritical speeds. Again, the waveform is periodic in nature. In the Jth order manifestation (that is, $J = 1, 2, 3, \ldots$) of supercritical spontaneous sidebanding, when the rotative speed is approximately $(J + 1)/J$ times the natural frequency, the dominant frequency is precisely $J/(J + 1)$ times the rotative speed, or approximately equal to the *natural frequency.* Once again, there appears to be transition zones between successive orders of J when the response has a dominant frequency approximately equal to the *natural frequency*

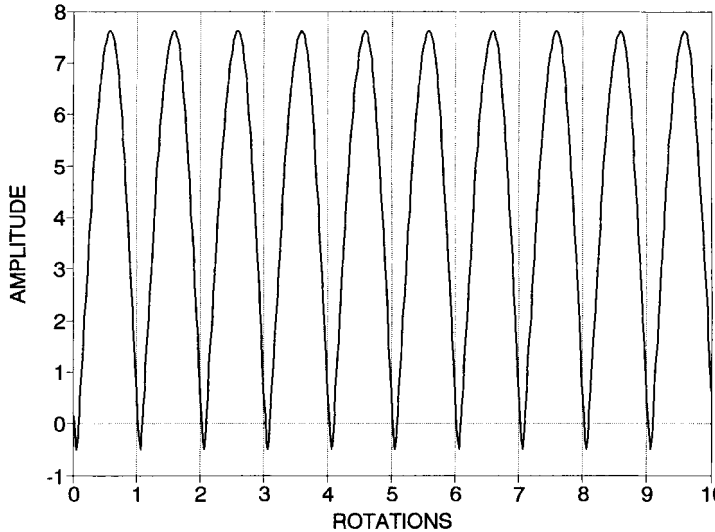

FIGURE 4.21 Critical synchronous resonant response—waveform ($z_1 = 0.200$; $\beta = 0.005$; $s = 1.050$).

and the waveform may be chaotic. Analogous to the general finding for subcritical ultra-subharmonic response, it has been noted[9] that such ultra-subharmonic response can be found in a speed range just above the Mth-order subharmonic peak at a rotational speed which is approximately $(MJ + 1)/J$ times the natural frequency (where $J = 1, 2, 3, \ldots$) with a dominant repsonse frequency precisely equal to $J/(MJ + 1)$ times the rotational speed.

Subharmonic Response.[10–14] The pseudo-critical peak at 2 times critical speeds shown in Fig. 4.17*A* exemplifies subharmonic response at supercritical speed. With a peak amplitude of the same order of magnitude as critical response, the rotor is bouncing at its natural frequency against the hard surface of the contact point as depicted in Fig. 4.22 and is subjected to the periodic component of the unbalance centrifugal force twice every bounce. Only one of the two pulses of unbalance force is effective in energizing the bouncing motion in the course of each bounce, so the dominant frequency of the response is then precisely one-half the operating speed. Such a pseudo-critical is possible for any integer order N at a rotational speed approximately N times critical speed and with a dominant frequency of precisely $1/N$ times operating speed or approximately the system *natural frequency.*

Transition between Successive Subharmonic Orders. The transition response between successive subharmonic orders is quite analogous to the transition response between successive superharmonic orders previously noted. In between the successive subharmonic response zones (i.e., between the Nth and $(N + 1)$th order subharmonic responses) there may occur a regime of irregular response. The response has been noted by many researchers to be chaotic,[1,15–22] as identified as Zone II in Fig. 4.17*A* and illustrated in Fig. 4.23*A*. The chaotic motion may be preceded on one side by a cascade of period-doubling bifurcations in the trace of peak amplitude Y_p, as suggested in Zone I of Fig. 4.17*A*. Another pattern of transition response is periodic in waveform. As shown in Zone III of Fig. 4.17*A*, instead of having an unending series

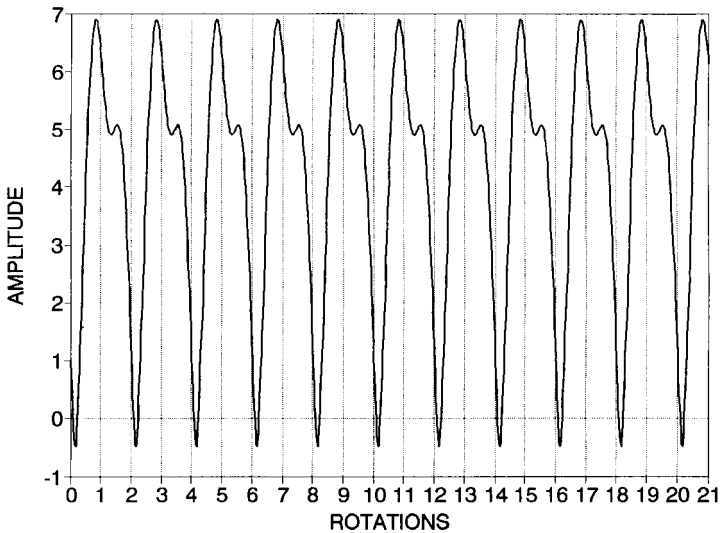

FIGURE 4.22 Supercritical subharmonic response—waveform ($z_1 = 0.200$; $\beta = 0.005$; $s = 2.150$; $N = 2$).

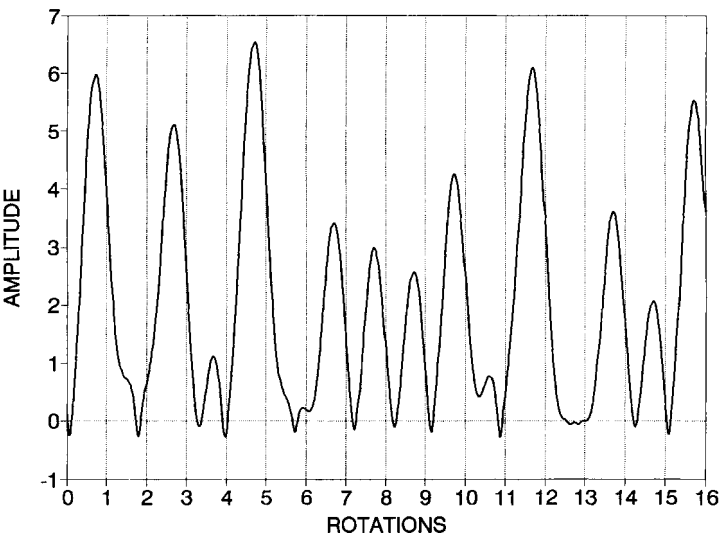

FIGURE 4.23*A* Supercritical chaotic transition between successive subharmonic orders—waveform ($z_1 = 0.200$; $\beta = 0.005$; $s = 1.600$; $1 < N < 2$).

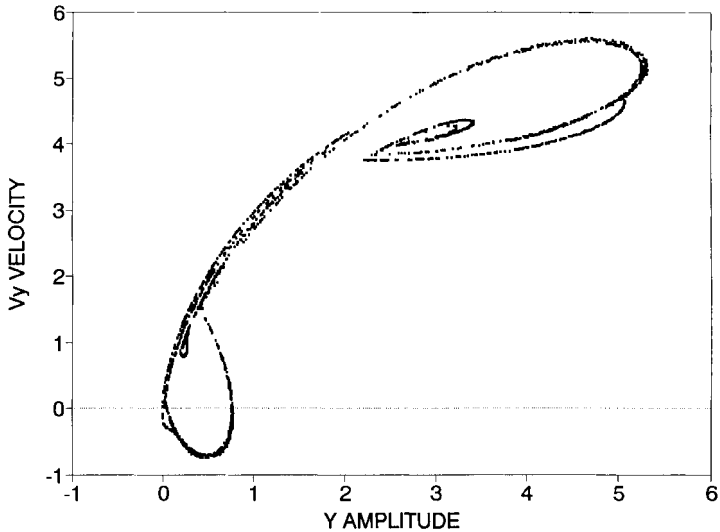

FIGURE 4.23*B* Supercritical chaotic transition between successive subharmonic orders—Poincaré section ($z_1 = 0.200$; $\beta = 0.005$; $s = 1.600$; $1 < N < 2$).

of local peaks with no identifiable periodicity of repetitions as would be the case in truly chaotic motion, the response appears to have clusters of K bounces that actually repeat every L rotations to give a major periodicity of K/L times s. In both the chaotic and periodic transition zones, the response has a significant component at or near the system's *natural frequency.* As with subcritical chaotic transition zones, a Poincaré section of chaotic motion in a supercritical chaotic transition zone is effectively a slice of the system's attractor as shown in Fig. 4.23*B*.

OTHER PHENOMENA

Self-Excited Vibration.* Consider the nonlinear equation of motion

$$m\ddot{x} + c(x^2 - 1)\dot{x} + kx = 0$$

This is known as Van der Pol's equation and may be written alternatively

$$\ddot{x} - \varepsilon(1 - x^2)\dot{x} + \kappa^2 x = 0 \tag{4.5}$$

The principal feature of this self-excited system resides in the damping term; for small displacements the damping is negative, and for large displacements the damping is positive. Thus, even an infinitesimal disturbance causes the system to oscillate; however, when the displacement becomes sufficiently large, the damping becomes positive and limits further increase in amplitude. This is shown in Fig. 4.24. Such systems, which start in a spontaneous manner, often are called *soft* systems in contrast with *hard* systems which exhibit sustained oscillations only if a shock in excess of a certain

* A general treatment of self-excited vibration is given in Chap. 5.

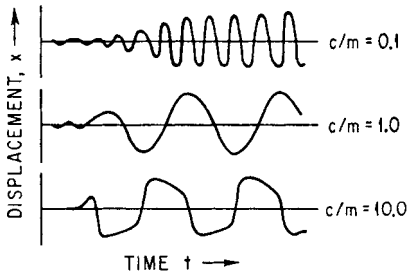

FIGURE 4.24 Displacement time-histories for Van der Pol's equation [Eq. (4.5)] for various values of the damping.

level is applied. Note that stability questions arise here (which are different from those discussed earlier in connection with jump phenomena) concerning the existence of one or more limiting amplitudes, such as the one noted above in the Van der Pol oscillator.

Relaxation Oscillations. As shown in Fig. 4.18, the motion of the Van der Pol oscillator is very nearly harmonic for $c/m = 0.1$ while the motion is made up of relatively sudden transitions between deflections of opposite sign for $c/m = 10.0$. The period of the harmonic motion for $c/m = 0.1$ is determined essentially by the linear spring stiffness k and the mass m; the period of the motion corresponding to $c/m = 10.0$ is very much larger and depends also on c. Thus, it is possible to obtain an undamped periodic oscillation in a damped system as a result of the particular behavior of the damping term. Such oscillations are often called *relaxation oscillations.*

Asynchronous Excitation and Quenching. In linear systems, the principle of superposition is valid, and there is no interaction between different oscillations. Moreover, the mathematical existence of a periodic solution always indicates the existence of a periodic phenomenon. In nonlinear systems, there is an interaction between oscillations; the mathematical existence of a periodic solution is only a necessary condition for the existence of corresponding physical phenomena. When supplemented by the condition of stability, the conditions become both necessary and sufficient for the appearance of the physical oscillation. Therefore, it is conceivable that under these conditions the appearance of one oscillation may either create or destroy the stability condition for another oscillation. In the first case, the other oscillation appears (*asynchronous excitation*), and in the second case, disappears (*asynchronous quenching*). The term *asynchronous* is used to indicate that there is no relation between the frequencies of these two oscillations.

Entrainment of Frequency. According to linear theory, if two frequencies ω_1 and ω_2 are caused to beat in a system, the period of beating increases indefinitely as ω_2 approaches ω_1. In nonlinear systems, the beats disappear as ω_2 reaches certain values. Thus, the frequency ω_1 falls in synchronism with, or is entrained by, the frequency ω_2 within a certain range of values. This is called *entrainment of frequency,* and the band of frequencies in which entrainment occurs is called the zone of entrainment or the interval of synchronization. In this region, the frequencies ω_1 and ω_2 combine and only vibration at a single frequency ensues.

EXACT SOLUTIONS

It is possible to obtain exact solutions for only a relatively few second-order nonlinear differential equations. In this section, some of the more important of these exact solutions are listed. They are exact in the sense that the solution is given either in closed form or in an expression that can be evaluated numerically to any desired degree of accuracy. Some general examples follow.

FREE VIBRATION

Consider the free vibration of an undamped system with a general restoring force $f(x)$ as governed by the differential equation

$$\ddot{x} + \kappa^2 f(x) = 0$$

This can be rewritten as

$$\frac{d(\dot{x}^2)}{dx} + 2\kappa^2 f(x) = 0 \tag{4.6}$$

and integrated to yield

$$\dot{x}^2 = 2\kappa^2 \int_x^X f(\xi)\, d\xi$$

where ξ is an integration variable and X is the value of the displacement when $\dot{x} = 0$. Thus

$$|\dot{x}| = \kappa\sqrt{2}\sqrt{\int_x^X f(\xi)\, d\xi}$$

This may be integrated again to yield

$$t - t_0 = \frac{1}{\kappa\sqrt{2}} \int_0^x \frac{d\zeta}{\sqrt{\int_\zeta^X f(\xi)\, d\xi}} \tag{4.7}$$

where ζ is an integration variable and t_0 corresponds to the time when $x = 0$. The displacement-time relation may be obtained by inverting this result. Considering the restoring force term to be an odd function, i.e.,

$$f(-x) = -f(x)$$

and considering Eq. (4.7) to apply to the time from zero displacement to maximum displacement, the period τ of the vibration is

$$\tau = \frac{4}{\kappa\sqrt{2}} \int_0^X \frac{d\zeta}{\sqrt{\int_\zeta^X f(\xi)\, d\xi}} \tag{4.8}$$

Exact solutions can be obtained in all cases where the integrals in Eq. (4.8) can be expressed explicitly in terms of X.

Case 1. Pure Powers of Displacement. Consider the restoring force function

$$f(x) = x^n$$

Equation (4.8) then becomes

$$\tau = \frac{4}{\kappa}\sqrt{\frac{n+1}{2}} \int_0^X \frac{d\zeta}{\sqrt{X^{n+1} - \zeta^{n+1}}}$$

Setting $u = \zeta/X$,

$$\tau = \frac{4}{\kappa\sqrt{X^{n-1}}}\left(\sqrt{\frac{n+1}{2}} \int_0^1 \frac{du}{\sqrt{1 - u^{n+1}}}\right)$$

The expression within the parentheses depends only on the parameter n and is denoted by $\psi(n)$. Thus

$$\tau = \frac{4}{\kappa\sqrt{X^{n-1}}}\ \psi(n) \tag{4.9}$$

The factor $\psi(n)$ may be evaluated numerically to any desired degree of accuracy, and is tabulated in Table 4.1.

Case 2. Polynomials of Displacement. Consider the binomial restoring force

$$f(x) = x^n + \mu x^m \qquad [m > n \geq 0]$$

Introducing this expression into Eq. (4.8) and performing the integrations:

$$\tau = \frac{4}{\kappa\sqrt{X^{n-1}}}\left(\sqrt{\frac{n+1}{2}}\int_0^1 \frac{du}{\sqrt{(1+\bar{\mu}) - (u^{n+1} + \bar{\mu}u^{m+1})}}\right) \tag{4.10}$$

where

$$\bar{\mu} = \mu X^{m-n}\left(\frac{n+1}{m+1}\right) \tag{4.11}$$

For particular values of n, m, and $\bar{\mu}$, the expression within the parentheses can be evaluated to any desired degree of accuracy by numerical methods. The extension of this method to higher-order polynomials can be made quite readily.

Case 3. Harmonic Function of Displacement. Consider now the problem of the simple pendulum which has a restoring force of the form

$$f(x) = \sin x$$

Introducing this relation into Eq. (4.7):

$$t - t_0 = \frac{1}{2\kappa}\int_0^x \frac{d\zeta}{\sqrt{\sin^2\frac{X}{2} - \sin^2\frac{\zeta}{2}}}$$

If $x = X$ and $t_0 = 0$, this integral can be reduced to the standard form of the complete elliptic integral of the first kind:

$$\hat{K}(\alpha) = \int_0^{\pi/2} \frac{dv}{\sqrt{1 - \sin^2\alpha\sin^2 v}} \tag{4.12}$$

Thus, the period of vibration is

$$\tau = \frac{1}{\kappa}\hat{K}\left(\frac{X}{2}\right) \tag{4.13}$$

The displacement-time function can be obtained by inversion and leads to the inverse elliptic functions. Replacing $\sin\alpha$ by U in Eq. (4.12), expanding by the binomial theorem, and then integrating yields Eq. (4.3).

Case 4. Velocity Squared Damping. As indicated by Eq. (4.6), the introduction of any other function of $\dot{x}^2$ does not complicate the problem. Thus, the differential equation*

* The ± sign is employed here, and elsewhere in this chapter, to account for the proper direction of the resisting force. Consequently, reference frequently is made to upper or lower sign rather than to plus or minus.

$$\ddot{x} \pm \frac{\delta}{2}\dot{x}^2 + \kappa^2 f(x) = 0$$

can be reduced to

$$\frac{d(\dot{x}^2)}{dx} \pm \delta\dot{x}^2 = 2\kappa^2 f(x)$$

Integrating the above equation,

$$\dot{x}^2 = 2\kappa^2 e^{\mp\delta x}\int_x^X e^{\pm\delta\xi} f(\xi)\, d\xi$$

Integrating again,

$$t = \int_{x_0}^{x} \frac{d\eta}{\dot{x}(\eta)}$$

where η is an integration variable.

FORCED VIBRATION

Exact solutions for forced vibration of nonlinear systems are virtually nonexistent, except as the system can be represented in a stepwise linear manner. For example, consider a system with a stepwise linear symmetrical restoring force characteristic, as shown in Fig. 4.4. Denote the lower of the two stiffnesses by k_1, the upper by k_2, and the displacement at which the change in stiffness occurs by x_1. Thus, the problem reduces to the solution of two linear differential equations:

$$m\ddot{x}' + k_1 x' = \pm P \sin \omega t \qquad [x_1 \geq x' \geq 0] \tag{4.14a}$$

$$m\ddot{x}'' + (k_1 - k_2)x_1 + k_2 x'' = \pm P \sin \omega t \qquad [x'' \geq x_1] \tag{4.14b}$$

where the upper sign refers to in-phase exciting force and the lower sign to out-of-phase exciting force. The appropriate boundary conditions are

$$\begin{aligned} x'(t=0) &= 0 \\ x'(t=t_1) &= x''(t=t_1) = x_1 \\ \dot{x}'(t=t_1) &= \dot{x}''(t=t_1) \\ \dot{x}''\left(t = \frac{\pi}{2\omega}\right) &= 0 \end{aligned} \tag{4.15}$$

The solutions of Eqs. (4.14) are

$$x' = \frac{\pm P/k_1}{1 - \omega^2/\omega_1^2}\sin \omega t + A_1 \cos \omega_1 t + B_1 \sin \omega_1 t$$

$$x'' = \frac{\pm P/k_2}{1 - \omega^2/\omega_2^2}\sin \omega t + A_2 \cos \omega_2 t + B_2 \sin \omega_2 t + \left(1 - \frac{k_1}{k_2}\right)x_1$$

where $\omega_1^2 = k_1/m$, $\omega_2^2 = k_2/m$, and the constants A_1, A_2, B_1, B_2 may be evaluated from the boundary conditions, Eq. (4.15).

This analysis also applies to the case of free vibration by setting $P = 0$. By assigning various values to k_1 and k_2, a wide variety of specific problems may be treated. It is not necessary to restrict the restoring forces to odd functions.

NUMERICAL METHODS AND CHAOTIC DYNAMICS

The advent of availability of high-speed digital computation in the 1960s has had a profound effect on the study of nonlinear vibrations, not only in the speed, efficiency, and extent of the solutions which were made available but also in the variety of problems that could be studied and the new phenomena that were discovered. The methodology is quite straightforward. A timewise integration of the equation or equations of motion is carried out using any appropriate numerical integration scheme—from the simplest trapezoidal format to more complex schemes such as that of Runge-Kutta. The criteria for selection of the integration scheme are dependent on:

1. *The nature of the solution being sought.* A solution that is expected to have sharp discontinuities in amplitude or velocity would suggest the use of a linear or very low-order polynomial fit implicit in the integration scheme.
2. *The efficiency of the solution scheme.* Complex schemes that require more calculation for each incremental step in time usually permit the use of longer steps and hence fewer steps for a given total time interval. Conversely, simpler schemes that require less calculation for each incremental step in time usually require the use of shorter steps and hence more steps for a given total time interval.

The final selection of integration scheme and the size of the time step is very often made on the basis of trial and error where the step is refined to smaller and smaller values until the successive solutions no longer show a dependence on step size.

In cases where the requirement is for the stabilized "steady-state" solution to a dynamics problem (rather that the transient solution from a prescribed set of initial conditions), another precaution must be taken in numerical solution. The solution must be run long enough so that the initial transient from an arbitrarily selected set of initial conditions has decayed to negligible value. Here again, actual trials are generally conducted to assure the stabilization of the solution to the required accuracy. The issue does represent an important limitation when solutions are sought for the behavior of systems with very low damping.

Other limitations of numerical methods relate to their similitude with the actual physical systems which they are intended to model:

1. Numerical integration techniques are generally ineffective in deriving solutions in regions where those solutions are unstable in the sense that they are physically not achievable (such as illustrated in Fig. 4.16*C*).
2. For systems that have multivalued solutions, the particular solution branch which is achieved on any particular trial is dependent on the conditions set for initiating the computation sequence.

CHAOTIC DYNAMICS

Perhaps the most fundamental impact of the digital computer on the field of nonlinear vibration had been to make possible the discovery and the elucidation of chaotic vibrations.[1,20]

Chaotic vibrations are characterized by an irregular or ragged waveform such as illustrated in Figs. 4.19*A* and 4.23*A*. Although there may be recurrent patterns in the waveform, they are not precisely alike, and they repeat at irregular intervals, so the motion is truly nonperiodic as is implied in Zone II of Figs. 4.17*A* and 4.17*B*. Indeed,

care must be taken in characterizing vibration as chaotic since there are irregular motions which mimic chaotic response but in which there *are* recurrent patterns which repeat at regular intervals, such as are implied in Zone III of Figs. 4.17*A* and 4.17*B*.

Another characteristic of chaotic vibration is that, if the numerical solution (and, presumably, the physical system it represents) is started twice at nearly identical initial conditions, the two solutions will diverge exponentially with time.

For all its irregularity, there is a certain basic structure and patternation implicit in chaotic vibration. As one can infer from the response curves of local peak amplitude for chaotic vibration shown in Zone II of Figs. 4.17*A* and 4.17*B,* the maximum amplitude is bounded.

A remarkable response behavior associated with chaotic vibration is the cascade of period-doubling bifurcations or tree-like structure in peak amplitude response curve (illustrated in Zone I of Figs. 4.17*A* and 4.17*B*) that may take place in the transition from simple periodic response to chaotic response.

But the most remarkable property of chaotic vibrations is evident in the Poincaré section of the motion, shown typically in Figs. 4.19*B* and 4.23*B*. The Poincaré section contains a large number of discrete points of velocity plotted as a function of displacement of the chaotic motion where the points are sampled *stroboscopically* with reference to a particular phase angle of the forcing periodic function. Rather than a random scatter of points, the Poincaré section generally reveals striking patterns. The Poincaré section is sometimes referred to as an *attractor.*

Chaotic vibration also differs from random motion in that the power frequency spectrum generally has distinct peaks rather than consisting of broadband noise. There will often be not only synchronous response peaks at the forcing function frequency as in the response of linear systems, but there will also be a significant asynchronous response peak or peaks at the system's natural frequency of frequencies.

APPROXIMATE ANALYTICAL METHODS

A large number of approximate analytical methods of nonlinear vibration analysis exist, each of which may or may not possess advantages for certain classes of problems. Some of these are restricted techniques which may work well with some types of equations but not with others. The methods which are outlined below are among the better known and possess certain advantages as to ranges of applicability.

Approximate analytical methods, while useful for yielding insights into basic mechanisms and relative influence of independent variables, have been largely displaced by numerical methods which are capable of giving very precise results for very much more complex models by exploiting the enormous power of modern computers.

DUFFING'S METHOD

Consider the nonlinear differential equation (known as Duffing's equation)

$$\ddot{x} + \kappa^2(x \pm \mu^2 x^3) = p \cos \omega t \tag{4.16}$$

where the ± sign indicates either a hardening or softening system. As a first approximation to a harmonic solution, assume that

$$x_1 = A \cos \omega t \tag{4.17}$$

and rewrite Eq. (4.16) to obtain an equation for the second approximation:

$$\ddot{x}_2 = -(\kappa^2 A \pm \tfrac{3}{4}\kappa^2\mu^2 A^3 - p)\cos \omega t - \tfrac{1}{4}\kappa^2\mu^2 A^3 \cos \omega t$$

This equation may now be integrated to yield

$$x_2 = \frac{1}{\omega^2}(\kappa^2 A \pm \tfrac{3}{4}\kappa^2\mu^2 A^3 - p)\cos \omega t + \tfrac{1}{36}\kappa^2\mu^2 A^3 \cos 3\omega t \tag{4.18}$$

where the constants of integration have been taken as zero to ensure periodicity of the solution.

This may be regarded as an iteration procedure by reinserting each successive approximation into Eq. (4.16) and obtaining a new approximation. For this iteration procedure to be convergent, the nonlinearity must be small; i.e., κ^2, μ^2, A, and p must be small quantities. This restricts the study to motions in the neighborhood of linear vibration (but not near $\omega = \kappa$, since A would then be large); thus, Eq. (4.17) must represent a reasonable first approximation. It follows that the coefficient of the cos ωt term in Eq. (4.18) must be a good second approximation and should not be far different from the first approximation.[23] Since this procedure furnishes the exact result in the linear case, it might be expected to yield good results for the "slightly nonlinear" case. Thus, a relation between frequency and amplitude is found by equating the coefficients of the first and second approximations:

$$\omega^2 = \kappa^2(1 \pm \tfrac{3}{4}\mu^2 A^2) - \frac{p}{A} \tag{4.19}$$

This relation describes the response curves, as shown in Fig. 4.14.

The above method applies equally well when linear velocity damping is included.

RAUSCHER'S METHOD[24]

Duffing's method considered above is based on the idea of starting the iteration procedure from the linear vibration. More rapid convergence might be expected if the approximations were to begin with free nonlinear vibration; Rauscher's method is based on this idea.

Consider a system with general restoring force described by the differential equation

$$\omega^2 x'' + \kappa^2 f(x) = p \cos \omega t \tag{4.20}$$

where primes denote differentiation with respect to ωt, and $f(x)$ is an odd function. Assume that the conditions at time $t = 0$ are $x(0) = A$, $x'(0) = 0$. Start with the free nonlinear vibration as a first approximation, i.e., with the solution of the equation

$$\omega_0^2 x'' + \kappa^2 f(x) = 0 \tag{4.21}$$

such that $x = x_0(\phi)$ (where $\omega t = \phi$) has the period 2π and $x_0(0) = A$, $x_0'(0) = 0$. Equation (4.21) may be solved exactly in the form of quadratures according to Eq. (4.7):

$$\phi = \phi_0(x) = \frac{\omega_0}{\kappa\sqrt{2}} \int_A^x \frac{d\zeta}{\sqrt{\int_\zeta^A f(\xi)\, d\xi}} \tag{4.22}$$

Since $f(x)$ is an odd function and noting that ωt varies from 0 to $\pi/2$ as x varies from 0 to A,

$$\frac{1}{\omega_0} = \frac{\sqrt{2}}{\kappa\pi} \int_0^A \frac{d\zeta}{\sqrt{\int_\zeta^A f(\xi)\, d\xi}} \tag{4.23}$$

With ω_0 and ϕ_0 determined by Eqs. (4.23) and (4.22), respectively, the next approximation may be found from the equation

$$\omega_1^2 x'' + \kappa^2 f(x) - p \cos \phi_0 = 0 \tag{4.24}$$

In the original differential equation, Eq. (4.20), ωt is replaced by its first approximation ϕ_0 and ω_0 (now known) is replaced by its second approximation ω_1, thus giving Eq. (4.24). This equation is again of a type which may be integrated explicitly; therefore, the next approximation ω_1 and ϕ_1 may be determined. In those cases where $f(x)$ is a complicated function, the integrals may be evaluated numerically.

This method involves reducing nonautonomous systems to autonomous ones* by an iteration procedure in which the solution of the free vibration problem is used to replace the time function in the original equation, which is then solved again for $t(x)$. The method is accurate and frequently two iterations will suffice.

THE PERTURBATION METHOD

In one of the most common methods of nonlinear vibration analysis, the desired quantities are developed in powers of some parameter which is considered small; then the coefficients of the resulting power series are determined in a stepwise manner. The method is straightforward, although it becomes cumbersome for actual computations if many terms in the perturbation series are required to achieve a desired degree of accuracy.

Consider Duffing's equation, Eq. (4.16), in the form

$$\omega^2 x'' + \kappa^2 (x + \mu^2 x^3) - p \cos \phi = 0 \tag{4.25}$$

where $\phi = \omega t$ and primes denote differentiation with respect to ϕ. The conditions at time $t = 0$ are $x(0) = A$ and $x'(0) = 0$, corresponding to harmonic solutions of period $2\pi/\omega$. Assume that μ^2 and p are small quantities, and define $\kappa^2\mu^2 \equiv \varepsilon, p \equiv \varepsilon p_0$. The displacement $x(\phi)$ and the frequency ω may now be expanded in terms of the small quantity ε:

$$\begin{aligned} x(\phi) &= x_0(\phi) + \varepsilon x_1(\phi) + \varepsilon^2 x_2(\phi) + \cdots \\ \omega &= \omega_0 + \varepsilon\omega_1 + \varepsilon^2\omega_2 + \cdots \end{aligned} \tag{4.26}$$

The initial conditions are taken as $x_i(0) = x_i'(0) = 0$ $[i = 1,2, \ldots]$.

Introducing Eq. (4.26) into Eq. (4.25) and collecting terms of zero order in ε gives the linear differential equation

$$\omega_0^2 x_0'' + \kappa^2 x_0 = 0$$

* An autonomous system is one in which the time *does not* appear explicitly, while a nonautonomous system is one in which the time *does* appear explicitly.

Introducing the initial conditions into the solution of this linear equation gives $x_0 = A \cos \omega t$ and $\omega_0 = \kappa$. Collecting terms of the first order in ε,

$$\omega_0^2 x_1'' + \kappa^2 x_1 - (2\omega_0\omega_1 A - \tfrac{3}{4}A^3 + p_0)\cos\phi + \tfrac{1}{4}A^3 \cos 3\phi = 0 \qquad (4.27)$$

The solution of this differential equation has a nonharmonic term of the form $\phi \cos \phi$, but since only harmonic solutions are desired, the coefficient of this term is made to vanish so that

$$\omega_1 = \frac{1}{2\kappa}\left(\tfrac{3}{4}A^2 - \frac{p_0}{A}\right)$$

Using this result and the appropriate initial conditions, the solution of Eq. (4.27) is

$$x_1 = \frac{A^3}{32\kappa^2}(\cos 3\phi - \cos\phi)$$

To the first order in ε, the solution of Duffing's equation, Eq. (4.25), is

$$x = A\cos\omega t + \varepsilon\frac{A^3}{32\kappa^2}(\cos 3\omega t - \cos\omega t)$$

$$\omega = \kappa + \frac{\varepsilon}{2\kappa}\left(\tfrac{3}{4}A^2 - \frac{p_0}{A}\right)$$

This agrees with the results obtained previously [Eqs. (4.18) and (4.19)]. The analysis may be carried beyond this point, if desired, by application of the same general procedures.

As a further example of the perturbation method, consider the self-excited system described by Van der Pol's equation

$$\ddot{x} - \varepsilon(1 - x^2)\dot{x} + \kappa^2 x = 0 \qquad (4.5)$$

where the initial conditions are $x(0) = 0, \dot{x}(0) = A\kappa_0$. Assume that

$$x = x_0 + \varepsilon x_1 + \varepsilon^2 x_2 + \cdots$$

$$\kappa^2 = \kappa_0^2 + \varepsilon\kappa_1^2 + \varepsilon^2\kappa_2^2 + \cdots$$

Inserting these series into Eq. (4.5) and equating coefficients of like terms, the result to the order ε^2 is

$$x = \left(2 - \frac{29\varepsilon^2}{96\kappa_0^2}\right)\sin\kappa_0 t + \frac{\varepsilon}{4\kappa_0}\cos\kappa_0 t + \frac{\varepsilon}{4\kappa_0}\left(\frac{3\varepsilon}{4\kappa_0}\sin 3\kappa_0 t - \cos 3\kappa_0 t\right) - \frac{5\varepsilon^2}{124\kappa_0^2}\sin 5\kappa_0 t \qquad (4.28)$$

THE METHOD OF KRYLOFF AND BOGOLIUBOFF[25]

Consider the general autonomous differential equation

$$\ddot{x} + F(x, \dot{x}) = 0$$

which can be rewritten in the form

$$\ddot{x} + \kappa^2 x + \varepsilon f(x, \dot{x}) = 0 \qquad [\varepsilon << 1] \qquad (4.29)$$

For the corresponding linear problem ($\varepsilon \equiv 0$), the solution is

$$x = A \sin(\kappa t + \theta) \tag{4.30}$$

where A and θ are constants.

The procedure employed often is used in the theory of ordinary linear differential equations and is known variously as the method of variation of parameters or the method of Lagrange. In the application of this procedure to a nonlinear equation of the form of Eq. (4.29), assume the solution to be of the form of Eq. (4.30) but with A and θ as time-dependent functions rather than constants. This procedure, however, introduces an excessive variability into the solution; consequently, an additional restriction may be introduced. The assumed solution, of the form of Eq. (4.30), is differentiated once considering A and θ as time-dependent functions; this is made equal to the corresponding relation from the linear theory (A and θ constant) so that the additional restriction

$$\dot{A}(t) \sin[\kappa t + \theta(t)] + \dot{\theta}(t) A(t) \cos[\kappa t + \theta(t)] = 0 \tag{4.31}$$

is placed on the solution. The second derivative of the assumed solution is now formed and these relations are introduced into the differential equation, Eq. (4.29). Combining this result with Eq. (4.31),

$$\dot{A}(t) = -\left(\frac{\varepsilon}{\kappa}\right) f[A(t) \sin \Phi, A(t)\kappa \cos \Phi] \cos \Phi$$

$$\dot{\theta}(t) = \frac{\varepsilon}{\kappa A(t)} f[A(t) \sin \Phi, A(t)\kappa \cos \Phi] \sin \Phi$$

where

$$\Phi = \kappa t + \theta(t)$$

Thus, the second-order differential equation, Eq. (4.29), has been transformed into two first-order differential equations for $A(t)$ and $\theta(t)$.

The expressions for $\dot{A}(t)$ and $\dot{\theta}(t)$ may now be expanded in Fourier series:

$$\begin{aligned} \dot{A}(t) &= -\left(\frac{\varepsilon}{\kappa}\right)\left\{K_0(A) + \sum_{n=1}^{r} [K_n(A) \cos n\Phi + L_n(A) \sin n\Phi]\right\} \\ \dot{\theta}(t) &= \frac{\varepsilon}{\kappa A}\left\{P_0(A) + \sum_{n=1}^{r} [P_n(A) \cos n\Phi + Q_n(A) \sin n\Phi]\right\} \end{aligned} \tag{4.32}$$

where

$$K_0(A) = \frac{1}{2\pi} \int_0^{2\pi} f[A \sin \Phi, A\kappa \cos \Phi] \cos \Phi \, d\Phi$$

$$P_0(A) = \frac{1}{2\pi} \int_0^{2\pi} f[A \sin \Phi, A\kappa \cos \Phi] \sin \Phi \, d\Phi$$

It is apparent that A and θ are periodic functions of time of period $2\pi/\kappa$; therefore, during one cycle, the variation of $\dot{A}$ and $\dot{\theta}$ is small because of the presence of the small parameter ε in Eqs. (4.32). Hence, the average values of $\dot{A}$ and $\dot{\theta}$ are consid-

ered. Since the motion is over a single cycle, and since the terms under the summation signs are of the same period and consequently vanish, then approximately:

$$\dot{A} \simeq -\left(\frac{\varepsilon}{\kappa}\right) K_0(A)$$

$$\dot{\theta} \simeq \frac{\varepsilon}{\kappa A} P_0(A)$$

$$\dot{\Phi} \simeq \kappa + \frac{\varepsilon}{\kappa A} P_0(A)$$

For example, consider Rayleigh's equation

$$\ddot{x} - (\alpha - \beta \dot{x}^2)\dot{x} + \kappa^2 x = 0 \tag{4.33}$$

By application of the above procedures:

$$\dot{A} = -\left(\frac{1}{\kappa}\right) K_0(A) = -\frac{1}{\kappa}\left[\frac{1}{2\pi}\int_0^{2\pi} (-\alpha + \beta A^2\kappa^2 \cos^2\Phi) A\kappa \cos^2\Phi \, d\Phi\right]$$

$$= \frac{A}{2}(\alpha - \tfrac{1}{4}\beta A^2\kappa^2) \tag{4.34}$$

Equation (4.34) may be integrated directly:

$$t = 2\int_{A_0}^{A} \frac{dA}{A(\alpha - \gamma A^2)} = \frac{1}{\alpha}\ln\frac{A^2}{\alpha - \gamma A^2}$$

Solving for A,

$$A = \frac{\alpha}{\gamma}\left[\frac{1}{1 + \left(\dfrac{\alpha}{\gamma A_0^2} - 1\right)e^{-\alpha t}}\right]^{1/2} \tag{4.35}$$

where

$$\gamma = \tfrac{3}{4}\beta^2\kappa^2 \tag{4.36}$$

The application of the method to Van der Pol's equation, Eq. (4.5), is easily accomplished and leads to a solution in the first approximation of the form similar to that of the perturbation solution given by Eq. (4.28).

THE RITZ METHOD

In addition to methods of nonlinear vibration analysis stemming from the idea of small nonlinearities and from extensions of methods applicable to linear equations, other methods are based on such ideas as satisfying the equation at certain points of the motion or satisfying the equation in the average. The Ritz method is an example of the latter method and is quite powerful for general studies.

One method of determining such "average" solutions is to multiply the differential equation by some "weight function" $\psi_n(t)$ and then integrate the product over a period of the motion. If the differential equation is denoted by E, this procedure leads to

$$\int_0^{2\pi} E\cdot\psi_n(t)\, dt = 0 \tag{4.37}$$

A second method of obtaining such average solutions can be derived from the calculus of variations by seeking functions that minimize a certain integral:

$$I = \int_{t_0}^{t_1} F(\dot{x}, x, t)\, dt = \text{minimum}$$

Consider a function of the form

$$\tilde{x}(t) = a_1\psi_1(t) + a_2\psi_2(t) + \cdots + a_n\psi_n(t)$$

where the $\psi_k(t)$ are prescribed functions. If $\tilde{x}$ is now introduced for x, then

$$I = I(a_1, a_2, \ldots, a_n)$$

and a necessary condition for I to be a minimum is

$$\frac{\partial I}{\partial a_1} = 0, \qquad \frac{\partial I}{\partial a_2} = 0, \ldots, \qquad \frac{\partial I}{\partial a_n} = 0 \tag{4.38}$$

This gives n equations of the form

$$\frac{\partial I}{\partial a_k} = \int_{t_0}^{t_1} \left(\frac{\partial F}{\partial \tilde{x}}\, \psi_k + \frac{\partial F}{\partial \dot{\tilde{x}}}\, \dot{\psi}_k \right) dt = 0 \tag{4.39}$$

for determining the n unknown coefficients. Integrating Eq. (4.39),

$$\frac{\partial I}{\partial a_k} = \left[\frac{\partial F}{\partial \dot{\tilde{x}}}\, \psi_k \right]_{t_0}^{t_1} + \int_{t_0}^{t_1} \left[\frac{\partial F}{\partial \tilde{x}} - \frac{d}{dt} \left(\frac{\partial F}{\partial \dot{\tilde{x}}} \right) \right] \psi_k\, dt = 0$$

The first term is zero because ψ_k must satisfy the boundary conditions; the expression in brackets under the integral in the second term is Euler's equation. The conditions given in Eqs. (4.38) then reduce to

$$\int_{t_0}^{t} E(\tilde{x})\psi_k\, dt = 0 \qquad [k = 1, 2, \ldots, n] \tag{4.40}$$

This is the same as Eq. (4.37); thus, it is not necessary to "know" the variational problem, but only the differential equation. The conditions given in Eqs. (4.40) then yield average solutions based on variational concepts.

Examples. As a first example of the application of the Ritz method, consider the equation

$$\ddot{x} + \kappa^2 x^n = 0$$

for which an exact solution was given earlier in this chapter [Eq. (4.9)]. Assume a single-term solution of the form

$$\tilde{x} = A \cos \omega t$$

The Ritz procedure, defined by Eq. (4.40), gives

$$\int_0^{2\pi} (-\omega^2 A \cos^2 \omega t + \kappa^2 A^n \cos^{n+1} \omega t)\, d(\omega t) = 0$$

from which

$$\frac{\omega^2}{\kappa^2} = \frac{4}{\pi} A^{n-1} \int_0^{\pi/2} \cos^{n+1} \omega t \, d(\omega t) = A^{n-1} \varphi(n) \tag{4.41}$$

The comparable exact solution obtained previously by introducing in Eq. (4.9) the quantity $2\pi/\omega$ for the period τ is

$$\frac{\omega^2}{\kappa^2} = \left[\frac{\pi^2/4}{\psi^2(n)} \right] X^{n-1} = \Phi(n) X^{n-1} \tag{4.42}$$

Values of $\varphi(n)$ from the approximate analysis and $\Phi(n)$ from the exact analysis are compared directly in Table 4.1, affording an appraisal of the accuracy of the method.

TABLE 4.1 Values of the Functions $\psi(n)$, $\Phi(n)$, $\varphi(n)$*

n	$\psi(n)$	$\Phi(n)$	$\varphi(n)$
0	1.4142	1.2337	1.2732
1	1.5708	1.0000	1.0000
2	1.7157	0.8373	0.8488
3	1.8541	0.7185	0.7500
4	1.9818	0.6282	0.6791
5	2.1035	0.5577	0.6250
6	2.2186	0.5013	0.5820
7	2.3282	0.4552	0.5469

* The mathematical expressions for $\psi(n)$, $\Phi(n)$, and $\varphi(n)$ and the equations to which they refer are:

$$\psi(n) = \sqrt{\frac{n+1}{2}} \int_0^1 \frac{du}{\sqrt{1-u^{n+1}}} \qquad \text{[Eq. (4.9)]}$$

$$\Phi(n) = \frac{\pi^2/4}{\psi^2(n)} \qquad \text{[Eq. (4.42)]}$$

$$\varphi(n) = \frac{4}{\pi} \int_0^{\pi/2} \cos^{n+1} \sigma \, d\sigma \qquad \text{[Eq. (4.41)]}$$

Consider now the nonautonomous system described by Duffing's equation

$$E \equiv \ddot{x} + \kappa^2(x + \mu^2 x^3) - p \cos \omega t = 0$$

Assuming

$$\tilde{x} = A \cos \phi, \qquad \phi = \omega t$$

the Ritz condition, Eq. (4.40), leads to

$$\int_0^{2\pi} \{[(1-\eta^2)A - s] \cos \phi + \mu^2 A^3 \cos^3 \phi\} \cos \phi \, d\phi$$

from which the amplitude-frequency relation is

$$(1 - \eta^2)A + \tfrac{3}{4}\mu^2 A^3 = \pm s \tag{4.43}$$

where

$$s = \frac{p}{\kappa^2}, \qquad \eta^2 = \frac{\omega^2}{\kappa^2} \tag{4.44}$$

The upper sign indicates vibration in phase with the exciting force. Equation (4.43) describes the response curves shown in Fig. 4.14*A* and corresponds to Eq. (4.19) obtained by Duffing's method.

Application of the Ritz method to Van der Pol's equation, Eq. (4.5), leads to the identical result given by Eq. (4.36).

GENERAL EQUATIONS FOR RESPONSE CURVES

The Ritz method has been applied extensively in studies of nonlinear differential equations. Some of the general equations for response curves thereby obtained are given here, both as a further example of the application of the method and as a collection of useful relations.

SYSTEM WITH LINEAR DAMPING AND GENERAL RESTORING FORCES

Consider a system with general elastic restoring force (an odd function) and described by the equation of motion

$$a\ddot{x} + b\dot{x} + cf(x) - P\cos\omega t = 0$$

A solution may be assumed in the form

$$\tilde{x} = A\cos(\omega t - \theta) = B\cos\phi + C\sin\phi \tag{4.45}$$

where $\phi = \omega t$, $B = A\cos\theta$, $C = A\sin\theta$. Introducing Eq. (4.45) according to the Ritz conditions, and recalling that $f(x)$ is to be an odd function,

$$\begin{aligned} -a\omega^2 A\cos\theta + b\omega A\sin\theta + cAF(A)\cos\theta &= P \\ -a\omega^2 A\sin\theta - b\omega A\cos\theta + cAF(A)\sin\theta &= 0 \end{aligned} \tag{4.46}$$

where

$$F(A) = \frac{1}{\pi A}\int_0^{2\pi} f(A\cos\sigma)\cos\sigma\, d\sigma$$

and σ is simply an integration variable.

Some algebraic manipulations with Eqs. (4.46) give independent equations for the two unknowns A and θ:

$$[F(A) - \eta^2]^2 + 4D^2\eta^2 = \left(\frac{s}{A}\right)^2 \tag{4.47}$$

$$\tan\theta = \frac{2D\eta}{F(A) - \eta^2} \tag{4.48}$$

where η^2 and s are defined according to Eq. (4.44) and

$$\kappa^2 = \frac{c}{a} \qquad p = \frac{P}{a} \qquad D = \frac{b}{2\sqrt{ac}}$$

Equation (4.47) describes response curves of the form shown in Fig. 4.15, and Eq. (4.48) gives the corresponding phase angle relationships. These two equations also yield other special relations which describe various curves in the response diagram:

Undamped free vibration curve (Fig. 4.13),

$$\eta^2 = F(A) \tag{4.49}$$

Undamped response curves (Fig. 4.14),

$$\eta^2 = F(A) \mp \frac{s}{A} \tag{4.50}$$

Locus of vertical tangents of undamped response curves (Fig. 4.17),

$$\eta^2 = F(A) + A\frac{\partial F(A)}{\partial A} \tag{4.51}$$

Damped response curves (Fig. 4.15),

$$\eta^2 = [F(A) - 2D^2] \mp \sqrt{\left(\frac{s}{A}\right)^2 - 4D^2[F(A) - D^2]} \tag{4.52}$$

Locus of vertical tangents of damped response curves (Fig. 4.17),

$$[F(A) - \eta^2]\left[F(A) + A\,\frac{\partial F(A)}{\partial A} - \eta^2\right] = -4D^2\eta^2 \tag{4.53}$$

The maximum amplitude of vibration is of interest. The amplitude at the point at which a response curve crosses the free vibration curve is termed the *resonance amplitude,* and is determined in the nonlinear case by solving Eqs. (4.49) and (4.52) simultaneously. This leads to

$$2D\eta = \frac{s}{A} \qquad \theta = \frac{\pi}{2} \tag{4.54}$$

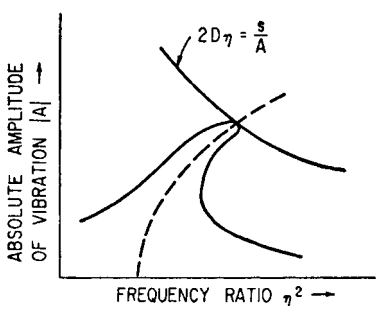

FIGURE 4.25 Determination of the resonant amplitude in accordance with Eq. (4.54).

The first of these two equations defines a hyperbola in the response diagram, describing the locus of crossing points, as shown in Fig. 4.25; hence, the intersection of this curve with the free vibration curve gives the resonance amplitude. The phase angle at resonance has the value $\pi/2$, as in the linear case. This result is of great help in computing response curves since the effect of damping (except for very large values) is negligible except in the neighborhood of resonance. Therefore, one may compute only the undamped curves (which is not difficult) and the hyperbola (which does not contain the nonlinearity); then, the effect of damping may be sketched in from knowledge of the crossing point.

SYSTEM WITH GENERAL DAMPING AND GENERAL RESTORING FORCES

The preceding analysis may be extended to include the more general differential equation

$$E \equiv \ddot{x} + 2D\kappa g(\dot{x}) + \kappa^2 f(x) - p\cos\omega t = 0$$

By procedures similar to those employed above:

$$[F(A) - \eta^2]^2 + 4D^2S^2(A) = \left(\frac{s}{A}\right)^2 \tag{4.55}$$

$$\tan\theta = \frac{2DS(A)}{F(A) - \eta^2} \tag{4.56}$$

where $$S(A) = \frac{1}{\pi\kappa A}\int_0^{2\pi} g(\omega A\sin\sigma)\sin\sigma\, d\sigma$$

In the case of linear velocity damping, $S(A) = \eta$, and Eqs. (4.55) and (4.56) reduce to Eqs. (4.47) and (4.48). The results for various types of damping forces are:

Coulomb damping:	$g(\dot{x}) = \pm\upsilon_0$	$S(A) = \frac{4}{\pi}\frac{\upsilon_0}{\kappa A}$
Linear velocity damping:	$g(\dot{x}) = \upsilon_1\dot{x}$	$S(A) = \upsilon_1\eta$
Velocity squared damping:	$g(\dot{x}) = \upsilon_2\dot{x}\lvert\dot{x}\rvert$	$S(A) = \frac{8}{3\pi}\upsilon_{2\eta}(A\omega)$
nth-power velocity damping:	$g(\dot{x}) = \upsilon_n\dot{x}\lvert\dot{x}\rvert^{n-1}$	$S(A) = \upsilon_{n\eta}(A\omega)^{n-1}\varphi(n)$

where $\varphi(n)$ is defined in Eq. (4.41) and values are given in Table 4.1.

The locus of resonance amplitudes or crossing points is now given by

$$2DS(A) = \frac{s}{A} \qquad \theta = \frac{\pi}{2}$$

GRAPHICAL METHODS OF INTEGRATION

Graphical methods (or their numerical equivalents) may be employed in the analysis of nonlinear vibration and often prove to be of great value both for general studies of the behavior of a particular system and for actual integration of the equation of motion.

A single degree-of-freedom system requires two parameters to describe completely the state of the motion. When these two parameters are used as coordinate axes, the graphical representation of the motion is called a *phase-plane* representation. In dealing with ordinary dynamical problems, these parameters frequently are taken as the displacement and velocity. First consider an undamped linear system having the equation of motion

$$\ddot{x} + \omega_n^2 x = 0 \tag{4.57}$$

and the solution

$$x = A\cos\omega_n t + B\sin\omega_n t$$
$$y = \frac{\dot{x}}{\omega_n} = -A\sin\omega_n t + B\cos\omega_n t \tag{4.58}$$

Eliminating time as a variable between Eqs. (4.58):

$$x^2 + y^2 = c^2$$

Thus, the phase-plane representation is a family of concentric circles with centers at the origin. Such curves are called *trajectories.* The necessary and sufficient conditions in the phase-plane for periodic motions are (1) closed trajectories and (2) paths described in finite time.

Now, suppose that the solution of Eq. (4.57) is not known. By introducing $y = \dot{x}/\omega_n$,

$$\frac{dx}{dt} = \omega_n y \qquad \frac{dy}{dt} = -\omega_n x$$

Therefore

$$\frac{dy}{dx} = -\frac{x}{y} \tag{4.59}$$

Thus, the path in the phase-plane is described by a simple first-order differential equation. This process of eliminating the time always can be done in principle, but frequently the problem is too difficult. Since the time is to be eliminated, *only autonomous systems can be treated by phase-plane methods.* When an equation of the type of Eq. (4.59) can be found, a direct solution of the problem follows since slopes of the trajectories can be sketched in the phase-plane and the trajectories determined by connecting the tangents; this is known as the method of *isoclines.* It sometimes happens that $dx = 0$, $dy = 0$ simultaneously so that there is no knowledge of the direction of the motion; such points in the phase-plane are called *singular points*. In the present example, the origin constitutes a singular point.

Consider now a damped linear system having the equation of motion

$$\ddot{x} + 2\zeta\omega_n\dot{x} + \omega_n^2 x = 0$$

and the solution

$$x = Ce^{-\delta t}\cos\Phi$$
$$y = \frac{\dot{x}}{\omega_n} = Ce^{-\delta t}\cos(\Phi + \sigma) \tag{4.60}$$

where

$$\delta = \zeta\omega_n = -\omega_n\cos\sigma \qquad \left[\sigma > \frac{\pi}{2}\right]$$
$$\Phi = \upsilon t + \theta$$
$$\upsilon = \omega_n\sqrt{1-\zeta^2} = \omega_n\sin\sigma$$

Equations (4.60) indicate that the trajectories in the phase-plane are some form of spiral (one of the simplest known of which is the logarithmic spiral). By referring to the oblique coordinate system shown in Fig. 4.26, and recalling that $\sin\sigma$ is a constant and

$$r^2 = x^2 + y^2 - 2xy\cos\sigma$$

Eqs. (4.60) reduce to

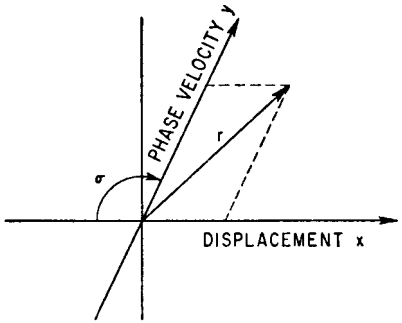

FIGURE 4.26 Phase-plane using oblique coordinates which results in a logarithmic spiral trajectory for a linear system with viscous damping [Eqs. (4.60)].

$$r = Ce^{-\delta t} \sin \sigma$$

This is a form of a logarithmic spiral.

The trajectories also could be found in a rectangular coordinate system, by the method of isoclines, without knowledge of the solution [Eqs. (4.60)]. The governing differential equation is

$$\frac{dy}{dx} = -\frac{2\zeta y + x}{y} \tag{4.61}$$

The resulting trajectories can be sketched in the phase-plane. On the other hand, Eq. (4.61) also can be integrated analytically by use of the substitution $z = y/x$ and separation of the variables:

$$y^2 + 2\zeta xy + x^2 = C \exp\left(\frac{2\zeta}{\sqrt{1-\zeta^2}} \tan^{-1} \frac{x\zeta + y}{x\sqrt{1-\zeta^2}}\right)$$

This is a spiral of the form of Eqs. (4.60).

The method of isoclines is extremely useful in studying the behavior of solutions in the neighborhood of singular points and for the related questions of stability of solutions. In this sense, phase-plane methods may be thought of as topological methods. However, it is desirable also to study the over-all solutions, rather than solutions in the neighborhood of special points, and preferably by some straightforward method of graphical integration. Such integration methods are given in the following sections of this chapter.

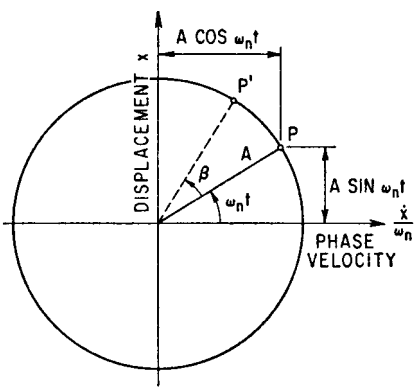

FIGURE 4.27 Phase-plane solution for a linear undamped vibrating system.

PHASE-PLANE INTEGRATION OF STEPWISE LINEAR SYSTEMS

Consider the undamped linear system described by Eq. (4.57). The known solution $x = A \sin \omega_n t, \dot{x} = A\omega_n \cos \omega_n t$ may be shown graphically in the phase-plane representation of Fig. 4.27. The point P moves with constant angular velocity ω_n, and the deflection increases to P' in the time β/ω_n.

If the system has a nonlinear restoring force composed of straight lines (as in Fig. 4.4), the motion within the region represented by any one linear segment can be described as above. For example, consider a system with the force-deflection characteristic shown at the top of Fig. 4.28. If the motion starts with initial velocity q_6 and zero initial deflection, the motion is described by a circular arc with center at 0 and angular velocity

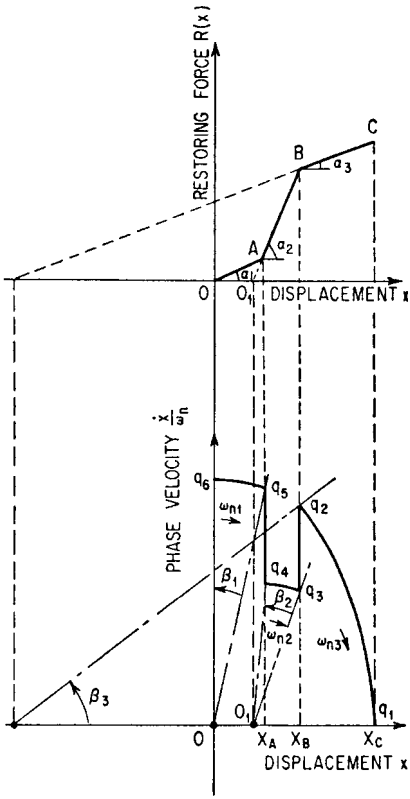

FIGURE 4.28 Phase-plane solution for the stepwise linear restoring force characteristic curve shown at the top. The motion starts with zero displacement but finite velocity.

$$\omega_{n_1} = \sqrt{\frac{1}{m}\tan\alpha_1}$$

from q_6 to q_5. At the point q_5, it is seen that $\dot{x}_A/\omega_{n_1} = \overline{x_A q_5}$ and $\dot{x}_A/\omega_{n_2} = \overline{x_A q_4}$. Therefore

$$\frac{\overline{x_A q_4}}{\overline{x_A q_5}} = \sqrt{\frac{\tan\alpha_2}{\tan\alpha_1}}$$

In this example, $\tan\alpha_1 < \tan\alpha_2$ so that $\overline{x_A q_4} < \overline{x_A q_5}$. The circular arc from q_4 to q_3 corresponds to the segment AB of the restoring force characteristic with center at the intersection 0_1 of the segment (extended) with the X axis. The radius of this circle is $\overline{0_1 q_4}$, where

$$q_4 = \frac{\dot{x}_B}{\omega_{n_2}} \qquad \text{and} \qquad \omega_{n_2} = \sqrt{\frac{1}{m}\tan\alpha_2}$$

The total time required to go from q_6 to q_1 is

$$t = \frac{\beta_1}{\omega_{n_1}} + \frac{\beta_2}{\omega_{n_2}} + \frac{\beta_3}{\omega_{n_3}}$$

For a symmetrical system this is one-quarter of the period.

If the force-deflection characteristic of a nonlinear system is a smooth curve, it may be approximated by straight line segments and treated as above. It should be noted that the time required to complete one cycle is strongly influenced by the nature of the curve in regions where the velocity is low; therefore, linear approximations near the equilibrium position do not greatly affect the period.

The time-history of the motion (i.e., the x,t representation) may be obtained quite readily by projecting values from the X axis to an x,t plane.

Inasmuch as phase-plane methods are restricted to autonomous systems, only free vibration is discussed above. However, if a constant force were to act on the system, the nature of the vibration would be unaffected, except for a displacement of the equilibrium position in the direction of the force and equal to the static deflection produced by that force. Thus, the trajectory would remain a circular arc but with its center displaced from the origin. Therefore, *nonautonomous systems may be treated by phase-plane methods, if the time function is replaced by a series of stepwise constant values.* The degree of accuracy attained in such a procedure depends only on the number of steps assumed to represent the time function.

A system having a bilinear restoring force and acted upon by an external stepwise function of time, treated by the method described above, is shown in Fig. 4.29. Phase-plane methods therefore offer the possibility of treating transient as well as free vibrations.

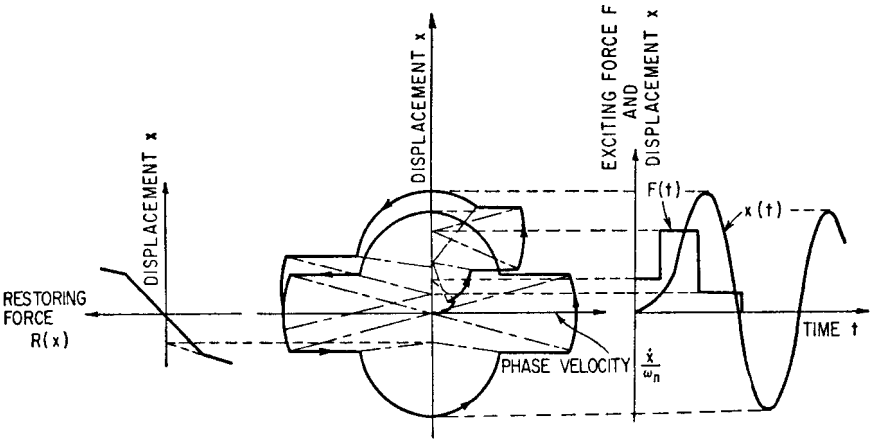

FIGURE 4.29 Phase-plane solution for transient motion. The bilinear restoring force characteristic curve is shown at the left, and the exciting force $F(t)$ and the resulting motion of the system $X(t)$ are shown at the right.

Phase-plane methods have been widely used for the analysis of control mechanisms.

PHASE-PLANE INTEGRATION OF AUTONOMOUS SYSTEMS WITH NONLINEAR DAMPING

Consider the differential equation

$$\ddot{x} + g(\dot{x}) + \kappa^2 x = 0$$

Introducing $y = \dot{x}/\kappa$, the following isoclinic equation is obtained:

$$\frac{dy}{dx} = -\frac{g(y) + x}{y} \tag{4.62}$$

For points of zero slope in the phase-plane, the numerator of Eq. (4.62) must vanish; therefore, the condition for zero slope is

$$x_0 = -g(y)$$

Points of infinite slope correspond to the X axis. Singular points occur where the x_0 curve intersects the X axis.

To construct the trajectory, the slope at any point P_i must be determined first. This is done as illustrated in Fig. 4.30: A line is drawn parallel to the X axis through P_i. The intersection of this line with the x_0 curve determines a point S_i on the X axis. With S_i as the center, a circular arc of short length is drawn through P_i; the tangent to this arc is the required slope. The termination of this short arc may be taken as the point P_{i+1}, etc. The accuracy of the construction is dependent on the lengths of the arcs. This construction is known as Liénard's method.

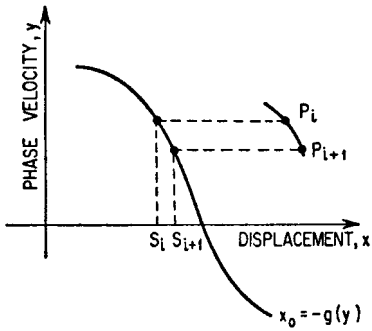

FIGURE 4.30 Liénard's construction for phase-plane integration of autonomous systems with nonlinear damping.

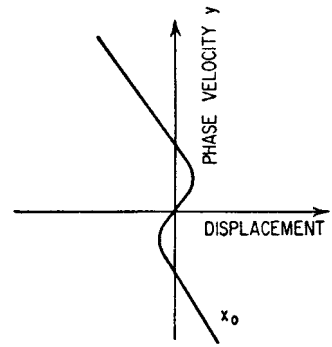

FIGURE 4.31 Curve of x_0 for Rayleigh's equation [Eq. (4.33)] as given by Eq. (4.63).

As an example of Liénard's method, consider Rayleigh's equation, Eq. (4.33), in the form

$$\ddot{x} + \varepsilon\left(\frac{\dot{x}^3}{3} - \dot{x}\right) + x = 0$$

The corresponding isoclinic equation is

$$\frac{dy}{dx} = \frac{\varepsilon(y - y^3/3) - x}{y}$$

The x_0 curve is given by

$$x_0 = \varepsilon\left(y - \frac{y^3}{3}\right) \tag{4.63}$$

This is illustrated in Fig. 4.31.

A little experimentation shows that if a point P_1 is taken near the origin, the slope is such as to take the trajectory away from the origin (as compared with the undamped vibration); by the same reasoning, a point P_2 far from the origin tends to take the trajectory toward the origin (again as compared with the undamped vibration). Therefore, there is some neutral curve, describing a periodic motion, toward which the trajectories tend; this neutral curve is called a *limit cycle* and is illustrated in Fig. 4.32. Such a limit cycle is obtained when x_0 has a different sign for different parts of the Y axis.

For extreme values of ε, the x_0 curves would appear as shown in Fig. 4.33. For $\varepsilon >> 1$, introduce the notation $\xi = x/\varepsilon$; then

$$\frac{dy}{d\xi} = \frac{\varepsilon}{y}\left(y - \frac{y^3}{3} - \xi\right)$$

This leads to a trajectory as shown in Fig. 4.34. This type of motion is known as a *relaxation oscillation.* Note from Fig. 4.34 that for this case of large ε the slope changes quickly from horizontal to vertical. Hence, for a motion starting at some point P_i, a vertical trajectory is followed until it intersects the ξ_0 curve; then, the trajectory turns and follows the ξ_0 curve until it enters the vertical field at the lower

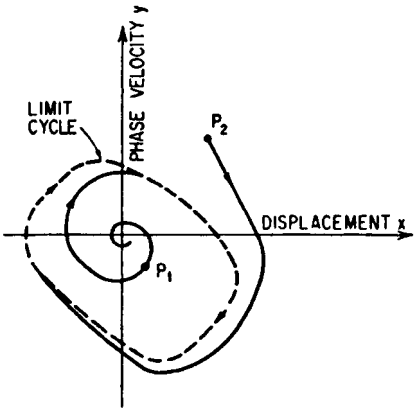

FIGURE 4.32 Limit cycle for Rayleigh's equation [Eq. (4.33)].

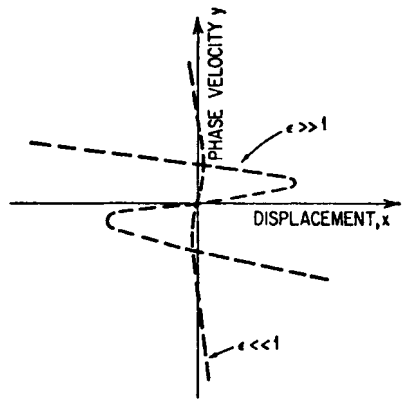

FIGURE 4.33 Curves of x_0 for extreme values of ε in Rayleigh's equation [Eq. (4.33)]. See Fig. 4.31 for a solution with a moderate value of ε.

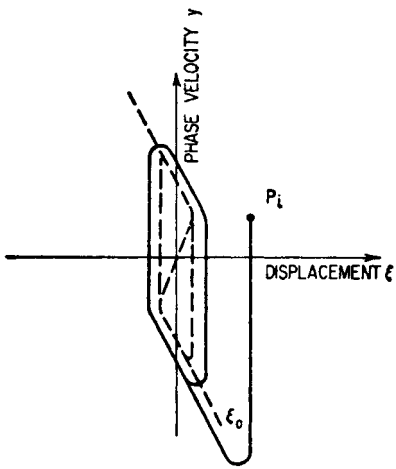

FIGURE 4.34 Relaxation oscillations of Rayleigh's equation [Eq. (4.33)].

knee in the curve. The trajectory then moves straight up until it intersects ξ_0 again after which it swings right and down again. A few circuits bring the trajectory into the limit cycle.

There is a possibility that more than one limit cycle may exist. If the x_0 curve crosses the X axis more than three times, it can be shown that at least two limit cycles may exist.

GENERALIZED PHASE-PLANE ANALYSIS

The following method of integrating second-order differential equations by phase-plane techniques has general application. Consider the general equation

$$\ddot{x} + F(x,\dot{x},t) = 0 \tag{4.64}$$

Equation (4.64) can be converted to the form

$$\ddot{x} + \kappa^2 x = g(x,\dot{x},t)$$

by adding $\kappa^2 x$ to both sides where

$$\kappa^2 x - F(x,\dot{x},t) = g(x,\dot{x},t)$$

Let

$$g(x_0,\dot{x}_0,t_0) = -\kappa^2 \Delta_0$$

where κ is chosen arbitrarily. At some point P_0 on the trajectory,

$$\ddot{x} + \kappa^2(x + \Delta_0) = 0$$

and

$$\frac{dy}{dx} = -\frac{x + \Delta_0}{y}$$

Referring to Fig. 4.35,

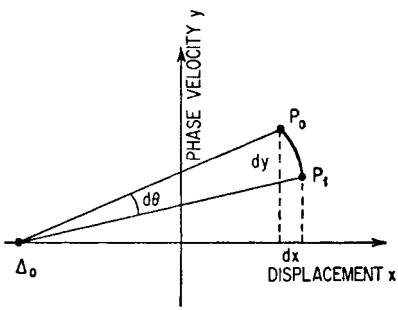

FIGURE 4.35 Method of construction employed in the generalized phase-plane analysis.

$$dt = \frac{1}{\kappa}\frac{dx}{y} = \frac{1}{\kappa}d\theta$$

Therefore, the time may be obtained by integration of the angular displacements. Thus, at a nearby point P_1 on the trajectory:

$$x_1 = x_0 + dx$$

$$y_1 = y_0 + dy$$

$$t_1 = t_0 + dt$$

Now, compute Δ_1 for the new center, and repeat the process.

This method has been applied to a very wide variety of linear and nonlinear equations. For example, Fig. 4.36 shows the solution of Bessel's equation

$$\ddot{x} + \frac{1}{t}\dot{x} + \left(p^2 - \frac{n^2}{t^2}\right)x = 0$$

of order zero. The angle (or time) projection of x yields $J_0(pt)$, while the $\dot{x}/p$ projection yields $J_1(pt)$; that is, the Bessel functions of the zeroth and first order of the first kind. Bessel functions of the second kind also can be obtained.

STABILITY OF PERIODIC NONLINEAR VIBRATION

Certain systems having nonlinear restoring forces and undergoing forced vibration exhibit unstable characteristics for certain combinations of amplitude and exciting frequency. The existence of such an instability leads to the "jump phenomenon" shown in Fig. 4.16. To investigate the stability characteristics of the response curves, consider Duffing's equation

$$\ddot{x} + \kappa^2(x + \mu^2 x^3) = p \cos \omega t \tag{4.65}$$

Assume that two solutions of this equation exist and have slightly different initial conditions:

$$x_1 = x_0$$

$$x_2 = x_0 + \delta \qquad [\delta << x_0]$$

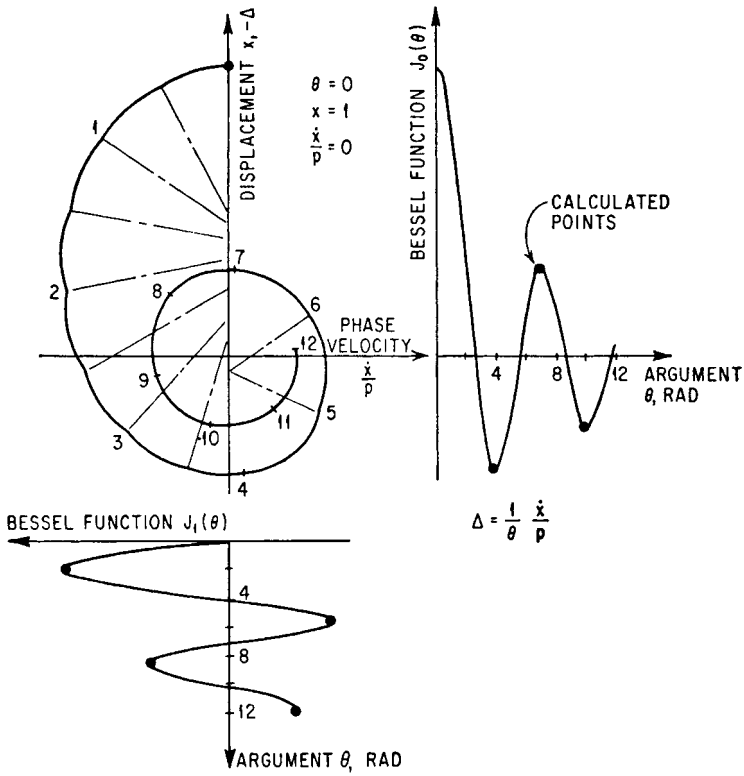

FIGURE 4.36 Generalized phase-plane solution of Bessel's equation.

Introducing the second of these into Eq. (4.65) and employing the condition that x_0 is also a solution,

$$\ddot{\delta} + \kappa^2(1 + 3\mu^2 x_0^2)\delta = 0 \tag{4.66}$$

Now an expression for x_0 must be obtained; assuming a one-term approximation of the form $x_0 = A \cos \omega t$, Eq. (4.66) becomes

$$\frac{d^2\delta}{d\varphi^2} + (\lambda + \gamma \cos \varphi)\delta = 0 \tag{4.67}$$

where
$$\kappa^2(1 + \tfrac{3}{4}\mu^2 A^2) = 4\omega^2\lambda$$

and
$$\tfrac{3}{4}\kappa^2\mu^2 A^2 = 4\omega^2\gamma \qquad 2\omega t = \varphi \tag{4.68}$$

Equation (4.67) is known as *Mathieu's equation.*

Mathieu's equation has appeared in this analysis as a variational equation characterizing small deviations from the given periodic motion whose stability is to be investigated; thus, the stability of the solutions of Mathieu's equation must be studied. A given periodic motion is stable if *all* solutions of the variational equation associated with it tend toward zero for all positive time and unstable if there is at least

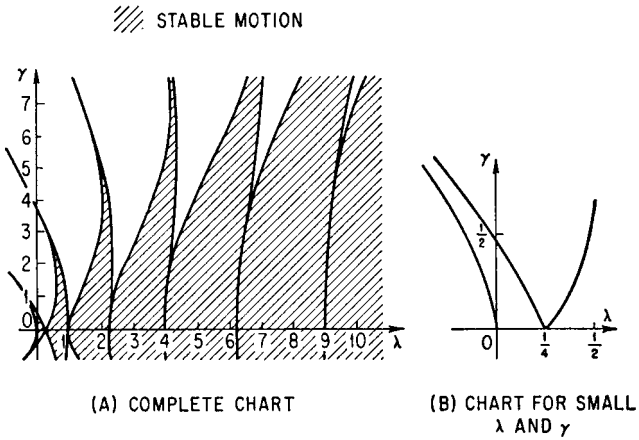

FIGURE 4.37 Stability chart for Mathieu's equation [Eq. (4.67)].

one solution which does not tend toward zero. The stability characteristics of Eq. (4.67) often are represented in a chart as shown in Fig. 4.37.

From the response diagram of Duffing's equation, the out-of-phase motion having the larger amplitude appears to be unstable. This portion of the response diagram (Fig. 4.16*C*) corresponds to unstable motion in the Mathieu stability chart (Fig. 4.37), and the locus of vertical tangents of the response curves (considering undamped vibration for simplicity) corresponds exactly to the boundaries between stable and unstable regions in the stability chart. Thus, the region of interest in the response diagram is described by the free vibration

$$\omega^2 = \kappa^2(1 + \tfrac{3}{4}\mu^2 A^2) \tag{4.69}$$

and the locus of vertical tangents

$$\tfrac{3}{2}\kappa^2\mu^2 A^2 + \frac{p}{A} = 0 \tag{4.70}$$

The corresponding curves in the stability chart are taken as those for small positive values of γ and λ which have the approximate equations

$$\gamma = \tfrac{1}{2} - 2\lambda \tag{4.71}$$

$$\gamma = -\tfrac{1}{2} + 2\lambda \tag{4.72}$$

Now, if Eq. (4.69) is introduced into Eqs. (4.68), the resulting equations expanded by the binomial theorem (assuming μ^2 small), and Eq. (4.72) introduced, the result is an identity. Therefore, the free vibration-response curve maps onto the curve of positive slope in the stability chart. The locus of vertical tangents to the response curves maps into the curve of negative slope in the stability chart; this may be seen from the identity obtained by introducing the equations obtained above by binomial expansion into Eq. (4.71) and then employing Eq. (4.70).

In any given case, it can be determined whether a motion is stable or unstable on the basis of the values of γ and λ, according to the location of the point in the stability chart.

The question of stability of response also can be resolved by means of a "stability criterion" developed from the Kryloff-Bogoliuboff procedures. The differential equation of motion is considered in the form

$$\ddot{x} + \kappa^2 x + f(x,\dot{x}) = p \cos \omega t$$

Proceeding in the manner of the Kryloff-Bogoliuboff procedure described earlier,

$$\dot{A} = \frac{1}{\kappa} f(x,\dot{x}) \sin(\kappa t + \theta) - \frac{p}{\kappa} \cos \omega t \sin(\kappa t + \theta)$$

$$\dot{\theta} = \frac{1}{\kappa} f(x,\dot{x}) \cos(\kappa t + \theta) - \frac{p}{A\kappa} \cos \omega t \cos(\kappa t + \theta)$$

Expanding the last terms of these equations, the result contains motions of frequency κ, $\kappa + \omega$, and $\kappa - \omega$. The motion over a long interval of time is of interest, and the motions of frequencies $\kappa + \omega$ and $\kappa - \omega$ may be averaged out; this is accomplished by integrating over the period $2\pi/\omega$:

$$\dot{A} = S(A) - \frac{p}{2\kappa} \sin(\Phi - \omega t)$$

$$\dot{\theta} = \frac{C(A)}{A} - \frac{p}{2\kappa A} \cos(\Phi - \omega t)$$

where

$$S(A) = \frac{1}{2\pi\kappa} \int_0^{2\pi} f(A \cos \Phi, -A\kappa \sin \Phi) \sin \Phi \, d\Phi$$

$$C(A) = \frac{1}{2\pi\kappa} \int_0^{2\pi} f(A \cos \Phi, -A\kappa \sin \Phi) \cos \Phi \, d\Phi$$

The steady-state solution may be determined by employing the conditions $A = A_0$, $\psi = \Phi - \omega t = \psi_0$:

$$\frac{p^2}{4\kappa^2} = S^2(A_0) + [C(A_0) + A_0(\kappa - \omega)]^2$$

$$\tan \psi_0 = \frac{S(A_0)}{C(A_0) + A_0(\kappa - \omega)}$$

This steady-state solution will now be perturbed and the stability of the ensuing motion investigated. Let

$$A(t) = A_0 + \xi(t) \qquad [\xi << A_0]$$

$$\psi(t) = \psi_0 + \eta(t) \qquad [\eta << \psi_0]$$

By Taylor's series expansion:

$$\dot{\xi} = \xi S'(A_0) - \frac{p}{2\kappa} \eta \cos \psi_0$$

$$\dot{\eta} = \frac{\xi}{A_0}[(\kappa - \omega) + C'(A_0)] + \frac{p}{2\kappa A_0} \eta \sin \psi_0$$

where primes indicate differentiation with respect to A. These two differential equations are satisfied by the solutions

$$\xi = \mathfrak{A} e^{zt} \qquad \eta = \mathfrak{B} e^{zt}$$

where $\mathfrak{A}$ and $\mathfrak{B}$ are arbitrary constants and

$$z = \frac{1}{2A_0}\left\{[S(A_0) + A_0S'(A_0)] \pm \sqrt{[S(A_0) + A_0S'(A_0)]^2 - 4A_0\bar{p}\,\frac{d\bar{p}}{dA_0}}\right\}$$

and $\bar{p} = p/2\kappa$.

For stability, the real parts of z must be negative; hence, the following criteria can be established:

$$[S(A_0) + A_0S'(A_0)] < 0,\ \frac{d\bar{p}}{dA_0} > 0, \text{ ensures stability}$$

$$[S(A_0) + A_0S'(A_0)] < 0,\ \frac{d\bar{p}}{dA_0} < 0, \text{ ensures instability}$$

$$[S(A_0) + A_0S'(A_0)] > 0,\ \frac{d\bar{p}}{dA_0} \gtrless 0, \text{ ensures instability}$$

$$[S(A_0) + A_0S'(A_0)] = 0,\ \frac{d\bar{p}}{dA_0} > 0, \text{ ensures stability}$$

These criteria can be interpreted in terms of response curves by reference to Fig. 4.14. For systems of this type, $[S(A_0) + A_0S'(A_0)] < 0$; when $d\bar{p}/dA_0 > 0$, $\bar{p}$ increases as A_0 also increases. This does not hold for the middle branch of the response curves, thus confirming the earlier results.

SYSTEMS OF MORE THAN A SINGLE DEGREE-OF-FREEDOM

Interest in systems of more than one degree-of-freedom arises from the problem of the dynamic vibration absorber. The earliest studies of nonlinear two degree-of-freedom systems were those of vibration absorbers having nonlinear elements.

The analysis of multiple degree-of-freedom systems can be carried out by various of the methods described earlier in this chapter and are generally completely analogous to those given here for the single degree-of-freedom system, with analogous results.

REFERENCES

1. Thompson, J. M. T., and H. B. Stewart: "Nonlinear Dynamics and Chaos," pp. 310–320, John Wiley & Sons, Inc., New York, 1987.
2. Ehrich, F. F.: "Stator Whirl with Rotors in Bearing Clearance," *J. of Engineering for Industry,* **89(B)**(3):381–390, 1967.
3. Ehrich, F. F.: "Rotordynamic Response in Nonlinear Anisotropic Mounting Systems," *Proc. of the 4th Intl. Conf. on Rotor Dynamics,* IFTOMM, 1–6, Chicago, September 7–9, 1994.
4. Ehrich, F. F.: "Nonlinear Phenomena in Dynamic Response of Rotors in Anisotropic Mounting Systems," *J. of Vibration and Acoustics,* **117(B):**117–161, 1995.
5. Choi, Y. S., and S. T. Noah: "Forced Periodic Vibration of Unsymmetric Piecewise-Linear Systems," *J. of Sound and Vibration,* **121**(3):117–126, 1988.

6. Ehrich, F. F.: "Observations of Subcritical Superharmonic and Chaotic Response in Rotordynamics," *J. of Vibration and Acoustics,* **114**(1):93–100, 1992.
7. Nayfeh, A. H., B. Balachandran, M. A. Colbert, and M. A. Nayfeh: "An Experimental Investigation of Complicated Responses of a Two-Degree-of-Freedom Structure," ASME Paper No. 90-WA/APM-24, 1990.
8. Ehrich, F. F.: "Spontaneous Sideband ing in High Speed Rotordynamics," *J. of Vibration and Acoustics,* **114**(4):498–505, 1992.
9. Ehrich, F. F., and M. Berthillier: "Spontaneous Sidebanding at Subharmonic Peaks of Rotordynamic Nonlinear Response," *Proceedings of ASME DETC '97,* Paper No. VIB-4041:1–7, 1997.
10. Ehrich, F. F.: "Subharmonic Vibration of Rotors in Bearing Clearance," ASME Paper No. 66-MD-1, 1966.
11. Bently, D. E.: "Forced Subrotative Speed Dynamic Action of Rotating Machinery," ASME Paper No. 74-Pet-16, 1974.
12. Childs, D. W.: "Fractional Frequency Rotor Motion Due to Nonsymmetric Clearance Effects," *J. of Eng. for Power,* 533–541, July 1982.
13. Muszynska, A.: "Partial Lateral Rotor to Stator Rubs," IMechE Paper No. C281/84, 1984.
14. Ehrich, F. F.: "High Order Subharmonic Response of High Speed Rotors in Bearing Clearance," *J. of Vibration, Acoustics, Stress and Reliability in Design,* **110**(9):9–16, 1988.
15. Masri, S. F.: "Theory of the Dynamic Vibration Neutralizer with Motion Limiting Stops," *J. of Applied Mechanics,* **39:**563–569, 1972.
16. Shaw, S. W., and P. J. Holmes: "A Periodically Forced Piecewise Linear Oscillator," *J. of Sound and Vibration,* **90**(1):129–155, 1983.
17. Shaw, S. W.: "Forced Vibrations of a Beam with One-Sided Amplitude Constraint: Theory and Experiment," *J. of Sound and Vibration,* **99**(2):199–212, 1985.
18. Shaw, S. W.: "The Dynamics of a Harmonically Excited System Having Rigid Amplitude Constraints," *J. of Applied Mechanics,* **52:**459–464, 1985.
19. Choi, Y. S., and S. T. Noah: "Nonlinear Steady-State Response of a Rotor-Support System," *J. of Vibration, Acoustics, Stress and Reliability in Design,* 255–261, July 1987.
20. Moon, F. C.: "Chaotic Vibrations," John Wiley & Sons, Inc., New York, 1987.
21. Sharif-Bakhtiar, M., and S. W. Shaw: "The Dynamic Response of a Centrifugal Pendulum Vibration Absorber with Motion Limiting Stops," *J. of Sound and Vibration,* **126**(2):221–235, 1988.
22. Ehrich, F. F.: "Some Observations of Chaotic Vibration Phenomena in High Speed Rotordynamics," *J. of Vibration and Acoustics,* **113**(1):50–57, 1991.
23. Duffing, G.: "Erzwungene Schwingungen bei veranderlicher Eigenfrequenz," F. Vieweg u Sohn, Brunswick, 1918.
24. Rauscher, M.: *J. of Applied Mechanics,* **5:**169, 1938.
25. Kryloff, N., and N. Bogoliuboff: "Introduction to Nonlinear Mechanics," Princeton University Press, Princeton, N.J., 1943.